Aspects of Black Holes in Anti-deSitter Space

by

SUNEETA VARADARAJAN

A THESIS IN PHYSICS

Presented to the University of Madras in Partial Fulfilment of the Requirements for the Degree of Doctor of Philosophy

JULY 2001

The Institute of Mathematical Sciences
C.I.T. Campus, Taramani,
Chennai 600 113 INDIA.

THE INSTITUTE OF MATHEMATICAL SCIENCES
C I T CAMPUS, TARAMANI, MADRAS 600 113, INDIA

Phone: (044) 254 1856, (044) 254 0588
(044)254 1049, (044)254 2050
Fax: (044)254 1586; Grams: MATSCIENCE
Telex: 041 8960 PCO IN PP WDT 20
E-Mail: trg@imsc.ernet.in

Prof. T. R. Govindarajan

CERTIFICATE

This is to certify that the Ph.D. thesis submitted by Suneeta Varadarajan to the University of Madras, entitled **Aspects of black holes in anti-deSitter space** is a record of bonafide research work done by her under my supervision. The research work presented in this thesis has not formed the basis for the award to the candidate of any Degree, Diploma, Associateship, Fellowship or other similar titles.

It is further certified that the thesis represents independent work by the candidate and collaboration when existed was necessitated by the nature and scope of problems dealt with.

T. R. Govindarajan

Prof. T. R. Govindarajan

July, 2001.

Thesis Supervisor

Acknowledgements

I owe, to all my teachers who made me feel the excitement of physics, the motivation for my wishing to do research in this field - in particular, I remember the late Dr. R.K. Popli.

In my years of working on this thesis and other problems, I have had the usual share of ups and downs. I am deeply indebted to my advisor, Prof. T.R. Govindarajan for understanding this, and for his encouragement and pragmatic advice at several crucial stages which have helped me work smoothly. I would also like to thank him for the various interesting discussions we have had, that have greatly benefitted me in my thesis work and otherwise.

I am very indebted to Prof. Romesh Kaul, from whom I have learnt a lot : in physics, and more importantly, from his style of approaching physics problems, which has shaped my own way of working to a great extent. I shall also always remember the most enjoyable discussions we have had, often at the cost of a forgotten lunch or tea!

I would like to thank Prof. Parthasarathi Majumdar, for his constant support and encouragement in all my years at the institute. I have benefitted from interacting with him at various stages, and also from his courses on Field Theory, which I was fortunate to attend.

It is difficult to mention here all the other fruitful discussions that have contributed in no small way to the thesis, and also to my understanding of the subject. However, I would like to thank, in particular, Prof. G. Date, Prof. N.D. Hari Dass and Prof. B. Sathiapalan, for sparing the time to clarify my numerous doubts, and also for their useful comments on the results that form a part of this thesis. I have also enjoyed several interesting discussions on aspects of black hole physics with my collaborator, Sachin Vaidya.

I would like to thank all the other members of the String Theory, QG journal club for some spirited academic interactions. I would especially like to thank Prof. S. Govindarajan, Prof. T. Jayaraman, Prof. S. Kalyana Rama and Prof. R. Ramachandran.

I shall cherish my various midnight academic sessions and walks to the

Besant Nagar beach with other graduate students, both past and present, talking about the charm of doing physics. I will particularly remember my interactions with P. Ramadevi, Saurya Das, Arundhati Dasgupta, Radhika Vathsan and K.R.S. Balaji.

I also owe thanks to all the other academic members of the institute for various courses they have taught and the stimulating academic atmosphere. I shall remember the library and office staff of the institute for helping me many a time in the last few years. I would particularly like to thank our Administrative Officer, Mr. Jayaraman for his invaluable administrative assistance.

Contents

Chapter 0

Abstract

The work of S.W.Hawking has revealed a deep relationship between the laws of thermodynamics and those of black hole mechanics. Classically, black holes obey laws that are similar to the laws of thermodynamics. A semi-classical analysis of black holes shows that they also radiate, with a thermal spectrum. These two facts together imply that the laws of black hole mechanics could indeed be thought of as laws of thermodynamics of black holes, where certain quantities associated with black holes could be identified with standard thermodynamic quantities. In particular, one-fourth of the area of the event horizon of a black hole would then be identified with the thermodynamic entropy associated with a black hole. A major test for any quantum theory of gravity is to account for the thermodynamic entropy in terms of microscopic states associated with a quantum description of the black hole. It has been shown that in computations of black hole entropy in many formulations of quantum gravity (like canonical gravity and string theory), the semiclassical Bekenstein-Hawking entropy formula is reproduced exactly. It has also been shown recently that for the $(3+1)$-dimensional Schwarzschild black hole in the canonical gravity formulation, the next-order correction to the semi-classical entropy is $-3/2\ \log A$, where A is the black hole horizon area. This correction has been reproduced in many string theory computations, and leads to the intriguing question of whether the next-order correction to the semi-classical entropy is also universal, and if so, what its origin is.

Another recent development has been the AdS/CFT conjecture [15] proposed in string theory. According to this proposal, the large N limit of a conformally invariant gauge theory in d dimensions is governed by string theory on the product of a $(d+1)$-dimensional anti-deSitter(AdS) space with a compact manifold. An important application of the AdS/CFT conjecture is in the context of black holes in anti-deSitter space. A study of supergravity in the background of an AdS black hole gives valuable information about strongly coupled gauge theories living on the boundary of the black hole spacetime.

In this thesis, we study some aspects of black holes in anti-deSitter (AdS) spacetimes. These black holes are solutions to the Einstein equations with a negative cosmological constant. The question of the microscopic origin of entropy can be posed for these black holes. For the case of the BTZ [6] black hole, which is an AdS black hole in $(2+1)$ dimensions, this question is easier to address, as gravity in $(2+1)$ dimensions can be rewritten as a Chern-Simons theory. The BTZ black hole thus offers an arena for studying the origin of the states accounting for the semi-classical entropy and of the next-order correction which also seems to be universal.

We look at the BTZ black hole in different formulations of Euclidean gravity in three dimensions. The semi-classical entropy of the BTZ black hole has been obtained earlier in Lorentzian and Euclidean formulations of gravity. However, the Lorentzian and Euclidean computations do not agree in the next-order correction term to the Bekenstein-Hawking entropy, which is surprising. The correction to the Bekenstein-Hawking entropy for the Lorentzian BTZ black hole has been computed by studying the Cardy formula for the growth of states of the asymptotic conformal field theory at the boundary of the black hole spacetime. It agrees with the correction to the semi-classical entropy originally obtained in the quantum geometry formalism for the $(3+1)$-d Schwarzschild black hole [7], and is $-3/2\ \log(Area)$, i.e it is proportional to the logarithm of the black hole area.

We derive an *exact* expression for the partition function of the

BTZ black hole in the Euclidean path integral approach. Our computation uses the formulation of three-dimensional gravity with a negative cosmological constant in terms of Chern-Simons theory. From the exact expression for the partition function, we show that for black holes with large horizon area, there is indeed a correction to the semi-classical entropy that is proportional to the logarithm of the area (horizon length in this case) with a coefficient $-3/2$ in agreement with the result for the Schwarzschild black hole obtained in the canonical gravity formalism. We find that in the context of the BTZ black hole, the right expression for the logarithmic correction comes from the modular invariance associated with the toral boundary of the black hole.

In this thesis, we also examine the BTZ black hole in the Ponzano-Regge-Turaev-Viro (PRTV) Euclidean lattice gravity formulation. We describe the BTZ black hole in this formulation and show that on considering all possible triangulations of the BTZ black hole keeping the horizon length fixed, the semi-classical Bekenstein-Hawking entropy is reproduced. The maximum contribution to the entropy comes from states at the horizon. We also comment on the next-order corrections to the entropy in this formulation.

Recent interest in the study of black holes in anti-deSitter space comes from the AdS/CFT conjecture - a study of supergravity fields in the black hole background gives information about a strongly coupled gauge theory on the boundary of the black hole spacetime. We focus on the computations of the spectrum of the dilaton field in supergravity in the background of the infinite mass limit of the AdS-Schwarzschild black hole in five dimensions. This spectrum matches with the scalar glueball spectrum of lattice QCD in three dimensions. We show that the correct self-adjointness analysis of the problem reveals that in addition to the modes that correspond to the glueball spectrum in QCD, there is a discrete infinity of modes which correspond to an imaginary mass for the glueball. Further, the mode frequencies corresponding to this discrete spectrum depend on a $U(1)$ parameter, the self-adjointness parameter, that labels the choice of boundary conditions at the horizon. We discuss the possible significance of these modes and of the self-adjointness parameter in the boundary theory.

We also study the time-independent ('zero') mode of the massless scalar field in various non-extremal black hole backgrounds. Again, a self-adjointness analysis of the operator corresponding to the zero mode solution suggests the presence of a non-trivial zero mode solution. This non-trivial zero mode is not seen for the extremal Reissner- Nordstrom black hole.

We also compute a particular class of non-equilibrium modes (quasi-normal modes) for the the dilaton in the AdS-Schwarzschild black hole background. Quasi-normal modes, espacially, the imaginary part of the lowest quasi-normal mode, give the time-scale of decay of the dilaton. The AdS/CFT correspondence, relates the perturbation of the black hole by the dilaton field to a change in the expectation value of the operator that couples to the dilaton in the Yang-Mills theory on the boundary due to a perturbation from the state of thermal equilibrium. The imaginary part of the lowest quasi-normal mode for the dilaton field gives the time-scale of return of the Yang-Mills theory back to thermal equilibrium.

We propose a novel method based on superpotentials for obtaining the quasi-normal modes of AdS black holes. We obtain the lowest quasi-normal mode of the $(2+1)$-dimensional BTZ black hole exactly. This is possible because the black hole potential belongs to a class of exactly solvable potentials, derived from a superpotential. *It is interesting to note that this is perhaps the only known case where the quasi-normal modes of a black hole can be found exactly.* The modes are proportional to the surface gravity of the black hole.

We propose a scheme by which the potential corresponding to a scalar field perturbation of any AdS black hole can be approximated by a potential series derived from a superpotential. We use this to compute the quasi-normal modes of the five dimensional AdS-Schwarzschild black hole. We also discuss the applications of our method and results.

Publications

[1] BTZ Black Hole Entropy from Ponzano-Regge Gravity;
with R. K. Kaul and T. R. Govindarajan, Mod. Phys. Lett. **A14**, 349 (1999).

[2] Horizon States for AdS Black Holes;
with T. R. Govindarajan and S. Vaidya, Nucl. Phys. **B583**, 291 (2000).

[3] Quasi-normal Modes of AdS black holes : A Superpotential Approach;
with T. R. Govindarajan, Class. Quant. Grav. **18**, 265 (2001).

[4] Logarithmic Correction to the Bekenstein-Hawking Entropy of the BTZ Black Hole;
with T. R. Govindarajan and R. K. Kaul, Class. Quant. Grav. **18**, 2877 (2001).

Chapter 1

Introduction

The study of black holes, which are predicted by Einstein's theory of gravitation, has resulted in interesting new connections between diverse areas of physics. Both classical and quantum aspects of black holes have been studied extensively. Black holes are believed to be a possible final outcome of a collapse of a star about a few times the mass of our sun. Stars like our sun are known to be well described by classical general relativity. Some of these classical aspects can be studied for black holes as well. However, a black hole is characterised by two important features :

- The presence of an event horizon, such that any object that falls into it is irretrievably lost to any observer outside the horizon.
- A singularity in spacetime, where all known physics is not valid. This singularity need not be a curvature singularity : it can also be a point beyond which analytic continuation of the spacetime produces closed timelike curves.

As we shall see, these two features necessitate the understanding of the *quantum* black hole, i.e a description of the black hole in a quantum theory of gravity.

In this chapter, we take a look at some of the classical and quantum aspects of black holes and see how they have fuelled the search for a quantum theory of gravity. We also present motivations for studying these properties for a specific class of black holes : black holes that asymptotically go to anti-deSitter spacetime. The recently proposed AdS/CFT conjecture in string theory implies that certain properties of black holes in anti-deSitter space are related to properties of strongly coupled gauge theories. We conclude the chapter with a brief review of the AdS/CFT conjecture and its implications.

1.1 Black Hole Thermodynamics

Research in black hole physics entered an exciting new phase in the 1970s when it was found that black holes obeyed certain laws that were similar to the laws of thermodynamics. Historically, the first step in this direction was the work of Hawking [1] who showed that the surface area of the event horizon of a black hole can never decrease in time. This is a purely geometric result and bears a superficial resemblance to the second law of thermodynamics, which states that the entropy never decreases in time. However, this and the fact that information is irretrievably lost as a body crosses the horizon led Bekenstein [2] to propose that there was an entropy associated with the black hole which was proportional to its horizon area. For stationary black holes, Bardeen, Carter and Hawking [3] derived laws of black hole mechanics analogous to the zeroth and first law of thermodynamics. The zeroth law states that there is a quantity associated with the black hole, called its surface gravity κ, that is a constant on the horizon. κ physically represents the acceleration at the horizon : it seems analogous to the temperature. The first law relates the change in the parameters M (mass), J (angular momentum) and A (horizon area) of a stationary black hole as it is perturbed. The variation in these quantities, to first order satisfies the following equation :

$$\delta M = \frac{1}{8\pi}\kappa A \; + \; \Omega\delta J \qquad (1.1)$$

where Ω is like the angular velocity of the horizon. This is in units with $G = c = \hbar = k = 1$. Together, all the results point to a strong similarity to the laws of thermodynamics. In the spirit of Bekenstein, it would be rather tempting to suggest that the black hole was indeed a thermodynamic object with an entropy proportional to its area, a temperature proportional to its surface gravity, and an internal energy proportional to its mass. However, there is a problem with such a suggestion : the classical black hole is a cold object, and could be thought of as being at zero temperature. Thus, the physical temperature of the black hole seems to have nothing to do with its surface gravity.

The justification for thinking of the laws of black hole mechanics as the laws of thermodynamics associated with black holes came with the startling discovery of Hawking [4] that black holes actually radiate. A semi-classical analysis of quantum fields in the black hole background shows that the black hole radiates with the thermal spectrum of a black body at a temperature proportional to the surface gravity. The analysis considers a free quantum field propagating in the background of a spacetime that is undergoing gravitational collapse to form a Schwarzschild black hole. The field is initially in its vacuum state prior to the collapse. However, the particle content of the field at late times is that of a perfect black body at a temperature $\frac{\kappa}{2\pi}$. Thus the surface gravity is indeed proportional to a meaningful temperature (called the Hawking temperature) that can be associated with the black hole. This also lends credence to the suggestion of Bekenstein that the physical entropy of the black hole is proportional to its area (and in fact is $A/4$). However, the entropy of a system that is macroscopically described by thermodynamics has a statistical mechanical origin in terms of microstates associated with the system. Thus, the natural question to ask is : What are the microscopic states associated with black hole entropy? The analogue of the thermodynamic description of a system seems to be the classical general relativistic description. To find out the microstates accounting for the black hole entropy, it is necessary to describe the black hole in a quantum theory of gravity. Black hole entropy has been a testing ground for candidate theories of quantum gravity. A variety of approaches to quantum gravity have reproduced the Bekenstein-Hawking entropy formula for the black hole, notably string theory [5] and canonical gravity [12, 13].

Another motivation for a quantum theory of gravity comes from the information loss paradox. For asymptotically flat black holes, the Hawking temperature increases as the mass of the black hole decreases. Therefore, a black hole will radiate away some of its mass through Hawking radiation, and this will increase its Hawking temperature. It will then radiate more, and finally evaporate away completely within a finite time. In the final stage of evaporation, the black hole has a very small size - of the order of the Planck length. Thus, the final stage of evaporation can only be described by a quantum theory of gravity. The black hole which is formed from gravitational collapse of matter, is initially in a pure state. However, after it has radiated and evaporated away, we are left with a mixed state. Since a pure state cannot evolve unitarily into a mixed state, we are faced with a paradox. It is hoped that the correct quantum theory of gravity may shed light on this issue.

1.2 Why study Anti-deSitter black holes ?

In this thesis, we study some aspects of black holes in anti-deSitter (AdS) spacetimes. These black holes are solutions to the Einstein equations with a negative cosmological constant and asymptotically tend to AdS spacetime. The reasons for studying AdS black holes are twofold. One has to do with the issue of black hole entropy, and the other has to do with the AdS/CFT correspondence presented in the following section.

As we saw, an important question that a quantum theory of gravity must address is the microstates accounting for black hole entropy. This is a difficult question to answer for black holes in $(3+1)$ dimensions, due to the non-trivial nature of gravity in $(3+1)$ dimensions. However, $(2+1)$ dimensional gravity is simpler and can be rewritten as a Chern-

Simons theory. There does indeed exist a black hole solution to $(2+1)$ dimensional gravity with a negative cosmological constant, the BTZ black hole [6], that asymptotically tends to anti-deSitter spacetime. The BTZ black hole offers an arena for studying the origin of the states accounting for the semi-classical entropy, and may clarify several open issues about black holes that have nothing to do with the actual number of spacetime dimensions the black hole is in. It has been shown that in computations of black hole entropy in many formulations of quantum gravity (like canonical gravity and string theory), the semiclassical Bekenstein-Hawking entropy formula is reproduced. It has also been shown recently that for the $(3+1)$-dimensional Schwarzschild black hole in the canonical gravity formulation, the next-order correction to the semi-classical entropy is $-3/2 \ \log A$ [7], where A is the black hole horizon area. This correction has been reproduced in many string theory computations [11], and leads to the intriguing question of whether the next-order correction to the semi-classical entropy is also universal, and if so, what its origin is. The BTZ black hole is also of interest in string theory : it arises naturally in the near-horizon geometry of stringy black holes - the near-horizon geometry of certain near-extremal four and five-dimensional black holes is a product of the BTZ black hole geometry and a compact manifold. The entropy of these black holes is the same as that of the BTZ black hole.

In chapter 2, we examine the BTZ black hole in a Euclidean *lattice* gravity formulation. It is hoped that this formulation might lead to a better picture of the states corresponding to the black hole entropy. We describe the BTZ black hole in the Ponzano-Regge-Turaev-Viro formulation [8, 9] and show that on considering all possible triangulations of the BTZ black hole keeping the horizon length fixed, the black hole entropy is proportional to the horizon area. The maximum contribution to the entropy comes from states at the horizon [10]. The expression for entropy has an arbitrary parameter. Its origin is similar to that of the Immirzi parameter that appears in the calculation of the entropy of the Schwarzschild black hole in $(3+1)-d$ in the framework of loop gravity [12], [13]. The entropy obtained by us is the familiar Bekenstein-Hawking expression for the same value of the arbitrary parameter as that of the Immirzi parameter in the $(3+1)-d$ calculation.

In chapter 3, we derive an *exact* expression for the partition function of the BTZ black hole in the Euclidean path integral approach [14]. Our computation uses the fact that three-dimensional gravity with a negative cosmological constant is described in terms of two $SU(2)$ Chern-Simons theories. Then, $SU(2)$ Wess-Zumino conformal field theories are naturally induced on the boundary. The quantum degrees of freedom corresponding to the entropy of the black hole are described by these conformal field theories. From the exact expression for the partition function, we show that for black holes with large horizon area, there is indeed a correction to the semi-classical entropy that is proportional to the logarithm of the area (horizon length in this case) with a coefficient $-3/2$ again in agreement with the result for a four dimensional black hole obtained in ref. [7]. We find that in the context of the BTZ black hole, the right expression for the logarithmic correction comes from the modular invariance associated with the toral boundary of the black hole.

Another important reason for studying AdS black holes has to do with the recently proposed AdS/CFT correspondence. An implication of the AdS/CFT conjecture in the context of AdS black holes is that a study of supergravity in the background of an AdS black hole gives valuable information about strongly coupled gauge theories living on the boundary of the black hole spacetime. In the next section, we take a brief look at the AdS/CFT conjecture and its applications.

1.3 The AdS/CFT correspondence

According to the AdS/CFT correspondence in string theory [15], string theory on the product of a $(d+1)$-dimensional anti-deSitter(AdS) space with a compact manifold gives information about the large N limit of a conformally invariant gauge theory in d dimensions. Here, N is related to the curvature of the AdS space.

To understand the motivations for the conjecture, we first look at a system of coincident D-branes and its connections to gauge theories.

In addition to strings, superstring theory contains soliton-like membranes of various internal dimensionalities called Dirichlet branes (or D-branes) [16]. A Dirichlet p-brane (or Dp-brane) is a $(p+1)$ dimensional hyperplane in $(9+1)$ dimensional space-time where open strings are allowed to end. For the end-points of such a string, the $(p+1)$ longitudinal coordinates satisfy the conventional free (Neumann) boundary conditions, while the $(9-p)$ coordinates transverse to the Dp-brane have the fixed (Dirichlet) boundary conditions; hence the origin of the term *Dirichlet* brane. A D-brane is essentially a non-perturbative object in string theory : the tension of the D-brane is proportional to $1/g_s$ where g_s is the string coupling constant. A fascinating feature of D-branes is that they naturally realize gauge theories on their world volume. If we consider N coincident Dp-branes, then there are N^2 different species of open strings because they can begin and end on any of the D-branes. These open strings have massless modes which describe the oscillations of the branes, a gauge field living on the brane and their fermionic partners. N^2 is the dimension of the adjoint representation of $U(N)$, and the low energy dynamics of the open strings is described by a maximally supersymmetric $U(N)$ gauge theory.

Now, if N is large, then the stack of Dp-branes is a heavy object embedded into a theory of closed strings which contains gravity. This macroscopic object will curve spacetime : it may be described by some classical metric and other background fields including the Ramond-Ramond $p+1$ form potential. Indeed, in supergravity which is the low energy limit of string theory, such brane solutions can be found, carrying the appropriate Ramond-Ramond charge. Thus, we have two very different descriptions of the stack of Dp-branes: one in terms of the $U(N)$ supersymmetric gauge theory on its world volume, and the other in terms of the classical Ramond-Ramond charged p-brane background of the type II closed superstring theory.

The AdS/CFT conjecture is motivated by a study of the low energy effective action for string theory in the background of N coincident D3 branes. The D3-branes are extended along a $(3+1)$ dimensional plane in $(9+1)$ dimensional spacetime. There are both open string and closed string perturbative excitations. The closed string excitations are excitations of the empty space, and open string excitations are excitations of the D3-branes. In the low energy limit, the action has contributions from only the massless modes. The closed string massless states give a gravity supermultiplet in ten dimensions, and their low-energy effective action is that of type IIB supergravity. As we saw, the open string massless states are described by a low-energy effective action that is a $U(N)$ gauge theory - in fact, it is $\mathcal{N}=4$ $U(N)$ super Yang-Mills theory. The complete low-energy effective action is the sum of the actions for two decoupled systems, type IIB supergravity in the bulk, and $\mathcal{N}=4$ $U(N)$ super-Yang-Mills theory on the brane.

Considering the D3 brane system from a different point of view as a solution of supergravity, again the low energy theory consists of two decoupled pieces - bulk supergravity, and excitations of the near-horizon geometry of the brane system, which is $AdS_5 \times S^5$. Since in both descriptions, one of the decoupled pieces is bulk supergravity, the conjecture identifies the second piece that appears in the two cases. With this identification, the conjecture in its strong form implies that $\mathcal{N}=4$ U(N) super-Yang-Mills theory in $(3+1)$ dimensions is dual to type IIB superstring theory on $AdS_5 \times S^5$. This means that the Yang-Mills theory at the boundary effectively sums over all spacetimes which are asymptotic to $AdS_5 \times S^5$, and correspond to different situations like gravitons, fundamental string states, D-branes, black holes etc. An analysis reveals that the regime of small curvature in the anti-deSitter spacetime, where classical supergravity is a valid approximation, is related to *strongly* coupled Yang-Mills theory at the boundary of the spacetime. The strong form of the AdS/CFT conjecture, which is physically interesting, states that the two theories; $\mathcal{N}=4$ $U(N)$ super Yang-Mills theory in $(3+1)$ dimensions and type IIB superstring theory on $AdS_5 \times S^5$ are equivalent to each other for all values of the string coupling constant and

N. In its most general form, the conjecture also states a correspondence between string theory on any $(d+1)$ dimensional AdS space and an appropriate superconformal gauge theory on the d dimensional boundary of the space.

An intuitive way of seeing such a possible duality for $d = 4$ is as follows : $\mathcal{N} = 4$ $U(N)$ super Yang-Mills theory in $(3+1)$ dimensions is a conformally invariant theory. The conformal group in four dimensions is $SO(4,2)$, including the Poincare transformations, scale transformations and the special conformal transformations. The theory also has a global $SU(4)$ R-symmetry that rotates the six scalars and four fermions in the theory. Therefore, if it is dual to a string theory, the string theory must also reflect these symmetries. The easiest way by which this can happen is that the background geometry in which the strings propagate has $SO(4,2)$ as its isometry group. Such a background is five dimensional AdS space times a five-dimensional compact space. If the compact space is a five-sphere, we also obtain a $SO(6) \simeq SU(4)$ symmetry.

The AdS/CFT correspondence was stated in a way useful for physical applications by Witten [17]. Since in AdS spaces, infinity is timelike, a null geodesic can reach infinity in finite time. Interactions are not cut off at infinity, unlike for asymptotically flat spaces. Thus, natural physical observables are not scattering amplitudes which can be used only if there are well-defined asymptotic $|IN>$ and $|OUT>$ states. Instead, the relevant physical observables are correlators. From the AdS/CFT correspondence, these are correlators in the boundary CFT. In the limit of small curvature of the AdS space, string theory on AdS space can be approximated by classical supergravity. Supergravity fields in the bulk AdS spacetime are dual to operators in the boundary conformal theory. If ϕ is a field in the bulk, and $\mathcal{O}$ the corresponding boundary operator, then let $\phi \to \phi_0$ at the boundary of the AdS spacetime (rather, its conformal compactification). Then,

$$\left\langle \exp \int_{\mathbb{S}^d} \phi_0 \mathcal{O} \right\rangle_{CFT} = Z_S(\phi_0) \tag{1.2}$$

where $Z_S(\phi_0)$ is the supergravity partition function. For classical supergravity,

$$Z_S(\phi_0) \;=\; \exp(-I_S(\phi_0)) \qquad (1.3)$$

and $I_S(\phi)$ is the classical supergravity action. More generally, the r.h.s of (1.2) is a sum over classical supergravity partition functions on backgrounds that are asymptotically AdS and have the same boundary topology. With this interpretation, Witten [18] showed that for a particular choice of the boundary topology, one could have two such backgrounds : A thermal gas in AdS space, or an AdS-Schwarzschild black hole. For large value of the horizon radius, the black hole phase dominates; i.e the supergravity partition function for the black hole background is much larger than that for the gas in AdS space. However, for small horizon radii, it is the AdS gas phase that dominates. This is an example of the phase transition first discovered by Hawking and Page [19] in the context of four dimensional AdS black holes. It was argued by Witten [17] that with a choice of supersymmetry breaking boundary conditions at the boundary, the boundary theory is no longer superconformal Yang-Mills theory, but ordinary three-dimensional QCD. Then, the Hawking-Page phase transition in the bulk is dual to a confinement-deconfinement phase transition in the boundary QCD. The precise statement of the proposal was that supergravity on the *infinite mass limit* of the five-dimensional AdS-Schwarzschild black hole background could be related to the strongly coupled limit of three-dimensional non-supersymmetric QCD. There is strong evidence in favour of this proposal as supergravity on this background gives many of the features of strong coupling limit of QCD, like the area law behavior of Wilson loops, confinement, and the glueball mass spectrum with a mass gap.

In chapter 4, we focus on the supergravity computations that reproduce the glueball mass spectrum. The spectrum corresponding to the scalar glueball is reproduced by studying the dilaton field of supergravity in this black hole background. We study the time-independent *equilibrium* modes of the dilaton, which is a massless scalar field, in this background. The correct self-adjointness analysis of the problem reveals that in addition to the modes that correspond to the glueball spectrum in QCD, there is a discrete infinity of modes which correspond to an imaginary mass for the glueball. Further, the mode frequencies corresponding to this discrete spectrum depend on a $U(1)$ parameter, the self-adjointness parameter, that labels the choice of boundary conditions at the horizon. We discuss the possible significance of these modes and of the self-adjointness parameter in the boundary theory [20].

We also study the time-independent ('zero') mode of the massless scalar field in various non-extremal black hole backgrounds. The analysis is similar to the above case of the infinite mass limit of the five-dimensional AdS-Schwarzschild black hole. The self-adjointness analysis of the operator corresponding to the zero mode solution can be used to obtain a non-trivial zero mode solution peaked at the horizon. There is an infinite choice of boundary conditions again labelled by a U(1) parameter, all of which lead to the same zero-mode solution. Interestingly, this non-trivial zero mode is not seen for the extremal Reissner- Nordstrom black hole [20].

We have already stated the fact that a mode analysis of fields of supergravity in AdS black hole backgrounds reveals features of a strongly coupled gauge theory on the boundary. There is a very natural class of modes of fields in black hole backgrounds - quasi-normal modes - that have been extensively studied for asymptotically flat black holes. These are non-equilibrium modes, and correspond to modes with *ingoing* boundary conditions at the horizon. Thus they are characteristic modes associated with the decay of a perturbation of the black hole. They have been numerically computed for asymptotically flat black holes where they are of relevance in the context of gravitational wave detection.

For the dilaton field in an AdS black hole background, these modes (particularly, the imaginary part of the lowest quasi-normal mode) give the time-scale of decay of the dilaton. However, from the AdS/CFT correspondence, the perturbation of the black hole (by the dilaton field) implies a perturbation of the Yang-Mills theory (or rather, the expectation value of the operator that couples to the dilaton) at the boundary away from thermal equilibrium. Thus, the imaginary part of the lowest quasi-normal mode for the dilaton field gives the time-scale of return of the Yang-Mills theory back to thermal equilibrium.

In chapter 5, we propose a novel method, based on superpotentials for obtaining the quasi-normal modes of AdS black holes. We notice, that for the $(2+1)$-dimensional BTZ black hole, the exact analytic quasi-normal mode solutions can be obtained as the black hole potential belongs to a class of exactly solvable potentials, derived from a superpotential. This is perhaps the only known case where the quasi-normal modes of a black hole can be found *exactly*. The modes are proportional to the surface gravity of the black hole.

Based on analogy with the results for the $(2+1)$-dimensional BTZ black hole, we suggest that for the five-dimensional AdS-Schwarzschild black hole, the black hole potential can be described by a potential series derived from a superpotential - a truncation of the series at any finite order then represents the order of approximation to the exact potential in this scheme. The problem is then exactly solvable for any order and the form of the quasi-normal mode wave function is thus known. This is used as an ansatz to obtain the quasi-normal modes of the AdS_5-Schwarzschild black hole numerically. A convergence is seen in the values of the modes as the order of approximation is increased. This scheme (of approximation by exactly solvable potentials) can be used to compute quasi-normal modes for AdS black holes in any dimension [21].

In the concluding chapter, we summarise and discuss the results of the thesis. We also touch upon interesting future directions that seem to emerge from this work.

Chapter 2

The BTZ black hole in lattice gravity

In this chapter, we study the $(2+1)$-dimensional BTZ [6] black hole in detail and analyze the geometry of its Euclidean continuation. The BTZ black hole is a classical solution to Einstein gravity in spacetime with a negative cosmological constant. As is well-known, gravity in three spacetime dimensions is simple. For spacetime with a negative cosmological constant, the solutions to Einstein's equations are all locally spaces with constant negative curvature and differ from each other only in global identifications. The main motivation for studying the BTZ black hole is that the simple nature of gravity in three dimensions can be used to address questions related to the quantum properties of black holes which are difficult to answer for black holes in $(3+1)$ dimensions.

We use a lattice formulation of Euclidean gravity in three dimensions developed by Ponzano and Regge [8] and later modified by Turaev and Viro [9] (although it was used by Turaev and Viro to construct three-manifold invariants, and not as a formulation of lattice gravity). We first describe the formulation in detail. We then propose a picture of the BTZ black hole in this formulation and use it to compute the semi-classical entropy of this black hole. We discuss corrections to the entropy in this formulation.

2.1 The Lorentzian black hole

The Lorentzian BTZ black hole is a solution to gravity in $(2+1)$-dimensions with a negative cosmological constant $\Lambda = \frac{-1}{l^2}$. The action is

$$S = \frac{1}{16\pi G}\int \sqrt{-g}\left[R + 2l^{-2}\right] d^2x dt + B, \tag{2.1}$$

where B is a surface term that for the black hole solution, will be related to its mass and angular momentum. The Einstein field equation

$$R_{\mu\nu} - \frac{1}{2}g_{\mu\nu}(R + \frac{2}{l^2}) = 0 \tag{2.2}$$

is solved by the black hole solution described by the metric

$$ds^2 = -N^2 dt^2 + N^{-2}dr^2 + r^2(N^\phi dt + d\phi)^2 \tag{2.3}$$

where the lapse function $N(r)$ and the angular shift $N^\phi(r)$ are given by

$$\begin{aligned} N^2(r) &= -M + \frac{r^2}{l^2} + \frac{J^2}{4r^2} \\ N^\phi(r) &= -\frac{J}{2r^2} \end{aligned}$$

with $-\infty < t < \infty$, $0 < r < \infty$ and $0 \leq \phi \leq 2\pi$.

M and J appearing in (2.3) are the conserved charges associated with asymptotic invariance under time displacements (mass) and rotational invariance (angular momentum), respectively. These charges are given by flux integrals through a large circle at spacelike infinity.

The lapse function $N(r)$ vanishes for two values of r given by

$$r_\pm = l\left[\frac{M}{2}\left(1 \pm \sqrt{1 - \left(\frac{J}{Ml}\right)^2}\right)\right]^{1/2}. \tag{2.4}$$

Of these, r_+ is the black hole outer horizon. In order for the horizon to exist, one must have

$$M > 0, \quad |J| \leq Ml. \tag{2.5}$$

For the extremal black hole case $|J| = Ml$.

It is interesting to note here that with a simple coordinate transformation, the metric (2.3) reduces to that of anti-deSitter space. The black hole arises from anti-deSitter space by discrete identifications. For the BTZ black hole, the singularity at $r = 0$ is not a curvature singularity as the spacetime geometry of the black hole is one of constant negative curvature. It is a singularity in the causal structure - continuing past $r = 0$ brings in closed timelike curves. When the angular momentum of the black hole $J = 0$, there is, in addition, a singularity in the Hausdorff manifold structure of the spacetime at $r = 0$.

2.2 Euclidean continuation

The Euclidean continuation of the BTZ black hole [22] is obtained by writing $t = -i\tau$, $M_{Lor} = M$ and $J_{Lor} = iJ$. Then the metric

$$ds^2 = (N^\perp)^2 d\tau^2 + f^{-2} dr^2 + r^2 \left(d\phi + N^\phi d\tau\right)^2 \tag{2.6}$$

with

$$N^\perp = f = \left(-M + \frac{r^2}{\ell^2} - \frac{J^2}{4r^2}\right)^{1/2}, \qquad N^\phi = -iN^\phi_{\text{Lor}} = -\frac{J}{2r^2}. \tag{2.7}$$

We set

$$r_\pm{}^2 = \frac{M\ell^2}{2}\left[1 \pm \left(1 + \frac{J^2}{M^2\ell^2}\right)^{1/2}\right], \tag{2.8}$$

The coordinate transformation

$$x = \left(\frac{r^2 - r_+^2}{r^2 - r_-^2}\right)^{1/2} \cos\left(\frac{r_+}{\ell^2}\tau + \frac{|r_-|}{\ell}\phi\right) \exp\left\{\frac{r_+}{\ell}\phi - \frac{|r_-|}{\ell^2}\tau\right\}$$

$$
\begin{aligned}
y &= \left(\frac{r^2 - r_+^2}{r^2 - r_-^2}\right)^{1/2} \sin\left(\frac{r_+}{\ell^2}\tau + \frac{|r_-|}{\ell}\phi\right) \exp\left\{\frac{r_+}{\ell}\phi - \frac{|r_-|}{\ell^2}\tau\right\} \qquad (2.9)\\
z &= \left(\frac{r_+^2 - r_-^2}{r^2 - r_-^2}\right)^{1/2} \exp\left\{\frac{r_+}{\ell}\phi - \frac{|r_-|}{\ell^2}\tau\right\}
\end{aligned}
$$

takes the metric to the form of the metric for hyperbolic three-space $\mathcal{H}_3$. The metric becomes

$$
ds^2 = \frac{\ell^2}{z^2}(dx^2 + dy^2 + dz^2), \quad z > 0, \tag{2.10}
$$

Here we have set

$$
|r_-| = ir_- = \frac{J\ell}{2r_+} \tag{2.11}
$$

as from (2.8), r_- is pure imaginary. Changing to "spherical" coordinates

$$
\begin{aligned}
x &= R\cos\theta\cos\chi\\
y &= R\sin\theta\cos\chi \qquad (2.12)\\
z &= R\sin\chi
\end{aligned}
$$

with θ periodic, i.e.,

$$
(R, \theta, \chi) \sim (R, \theta + 2\pi, \chi). \tag{2.13}
$$

accounting for the periodicity of the Schwarzschild angular coordinate ϕ, we must make, in the new coordinates, the identifications

$$
(R, \theta, \chi) \sim (Re^{2\pi r_+/\ell}, \theta + \frac{2\pi|r_-|}{\ell}, \chi), \tag{2.14}
$$

The three dimensional Euclidean black hole may thus be described as the quotient of hyperbolic space $\mathcal{H}_3$ by the isometry (2.14). As in four dimensions, the Euclidean black hole corresponds to the region outside the event horizon of the Lorentzian solution. The topology of the Euclidean black hole is that of a solid torus, with the horizon a circle of radius r_+ at the core of the solid torus. r_- represents the amount of twist made before making the discrete identifications to obtain the solid torus.

2.3 Ponzano-Regge gravity

In this section, we study the lattice gravity approach of Ponzano and Regge [8] in three dimensions. The simplest notion of lattice gravity which avoids the use of coordinates was first proposed by Regge [23] in 1961. In Regge calculus, an n - dimensional curved Riemannian manifold is approximated by a collection of n-dimensional polyhedra. For e.g, a three-dimensional manifold is approximated by a collection of tetrahedra, where each tetrahedron is filled inside with flat space, and curvature can be thought of as being concentrated on the edges of tetrahedra. More precisely, since each edge of the tetrahedron separates two faces, the angle between the outward normals of two faces separated by the i-th edge, θ_i is the discrete analogue of curvature in this picture. A complete specification of the lengths of all the edges of the tetrahedra in the discretisation (called a *triangulation*) of the manifold carries the information that the metric carries in the continuum picture. The discrete analogue of the gravity action is then

$$S_{Regge} = \sum_i \theta_i \; l_i \tag{2.15}$$

where the sum is over all the edges in the triangulation.

In the lattice gravity approach of Ponzano and Regge [8] in three dimensions, a discrete analogue of the partition function for gravity is proposed. One first considers a triangulation, i.e a simplicial decomposition of the three-manifold M. Each three-simplex is a tetrahedron. To each edge of the tetrahedron, we assign a half-integral number j such that $(\sqrt{j(j+1)})$ is the discretized length of that edge. These lengths must of course satisfy the triangle inequalities corresponding to the triangular faces of the tetrahedron. It is seen that the Racah- Wigner $6j$ symbol which appears in the tensor product of SU(2) representations is also defined for a similar set of inequalities [1]. As was shown in [8], we can associate it with this 'coloured' tetrahedron - when the lengths are large, the $6j$ symbol is related to the Regge action for

[1]More details of $6j$ symbols and their properties can be found in Appendix 1

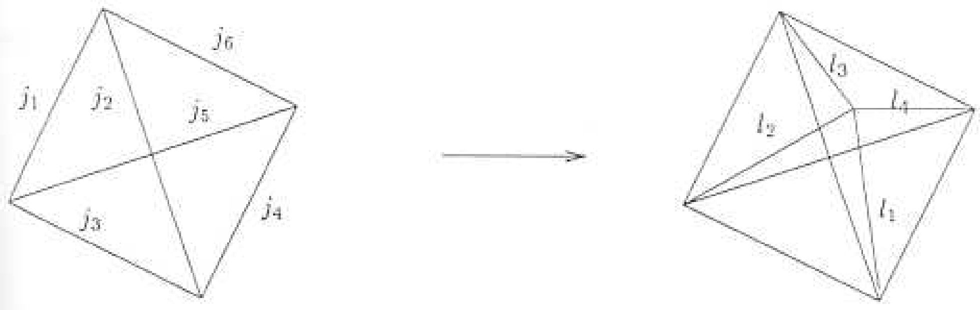

Figure 1. *Refinement of a tetrahedron into four tetrahedra*

a tetrahedron.

$$(-1)^{\sum_{i=1}^{6} j_i} \left\{ \begin{array}{ccc} j_1(t) & j_2(t) & j_3(t) \\ j_4(t) & j_5(t) & j_6(t) \end{array} \right\} \sim \frac{1}{\sqrt{12\pi V}} \cos(S_{Regge} + \pi/4) \quad (2.16)$$

Here, $S_{Regge} = \sum_{i=1}^{6} \theta_i \, (j_i + 1/2)$.

A partition function is constructed for the manifold M out of the various $6j$ symbols associated to the tetrahedra in the simplicial decomposition of M. In lattice gravity, one sums over geometries of the discretisation of M; in this picture, it corresponds to fixing a lattice structure and summing over all possible edge lengths. An important question to ask in any lattice approach is whether the model has a well-defined continuum limit. The continuum limit corresponds to refining the triangulation such that the discrete lattice starts approximating the smooth manifold M better and better.

The Ponzano-Regge partition function can be constructed to be invariant under refinement of any tetrahedron in the triangulation into four smaller tetrahedra. This process can be seen in Fig. 1. This scale invariance is achieved with an appropriate choice of weights in the partition function.

For a manifold without boundary, the partition function proposed by Ponzano and Regge is

$$
\begin{aligned}
Z_{PR} \; = \; & \sum_{colourings\ j_e \leq L} \; \prod_{vertices} \frac{1}{\Lambda} \prod_{e:\ edges} (2j_e+1) \quad \times \\
& \prod_{t:\ tetrahedra} \exp\left(-i\pi \sum_i j_i(t)\right) \left\{ \begin{array}{ccc} j_1(t) & j_2(t) & j_3(t) \\ j_4(t) & j_5(t) & j_6(t) \end{array} \right\}
\end{aligned} \tag{2.17}
$$

Here, the maximum spin value (maximum edge length) is cut off at L. For every vertex in the triangulation, a factor $1/\Lambda$ appears in the partition function. This regularizes the partition function as the limit $L \to \infty$ is taken. Λ is given by

$$
\Lambda(L) = \frac{1}{(2j_1+1)} \sum_{\substack{l_2, l_3 \leq L \\ |l_2 - l_3| \leq j_1 \leq l_2 + l_3}} (2l_2+1)(2l_3+1) \tag{2.18}
$$

It is shown in [24] that this partition function is the same as the partition function of ISO(3) Chern-Simons theory on the manifold M. The added knowledge that (2+1)-d gravity can be written as an ISO(2,1) Chern-Simons theory [25, 26] leads one to suspect that the Ponzano-Regge partition function might describe 3-d *Euclidean* gravity. The physical Hilbert space of Ponzano-Regge gravity is the same as that of the Chern- Simons theory. The physical Hilbert space of the Chern-Simons theory consists of coloured trivalent networks of Wilson lines. Each physical wave function in the basis of this Hilbert space is a homotopy class of such coloured trivalent networks. The exact relation of physical states of the Ponzano-Regge gravity to those of the Chern-Simons theory is obtained from the one-to-one correspondence between a homotopy class of coloured trivalent networks and a triangulation with colourings on the sides of the triangulation. A triangle in the Ponzano-Regge picture corresponds to a trivalent network as shown in Fig. 2. As can be seen, both are dual pictures. A tetrahedron corresponds to a dual tetrahedral spin network. This can be seen in Fig. 3.

Turaev and Viro showed [9] that there was a natural way of regularizing the Ponzano-Regge lattice sum - by considering the q-analogue of the model, where the spins are now associated with the quantum group

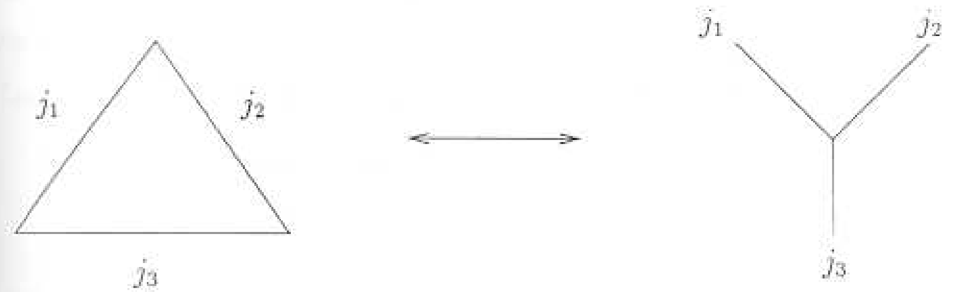

Figure 2. *A triangle and a dual trivalent spin network*

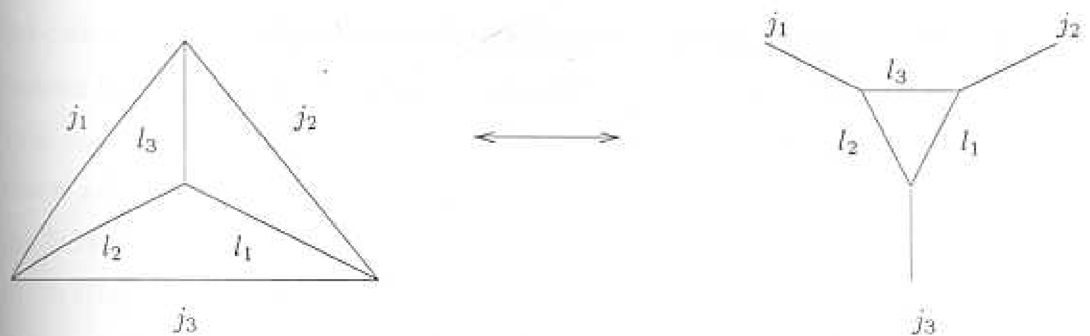

Figure 3. *A tetrahedron and dual tetrahedral spin network*

$U_q(SU(2))$ and $q = e^{\frac{2\pi i}{k+2}}$. k is an integer, and this leads to a natural cut-off on the maximum value of each spin, i.e $j \leq k/2$. In the partition function of Ponzano and Regge, ordinary numbers are replaced by q-numbers and ordinary $6j$ symbols by $SU(2)_q - 6j$ symbols. This choice of regularisation in fact corresponds to gravity with a cosmological constant.

The q-number of a number n is

$$[n]_q = \frac{q^{n/2} - q^{-n/2}}{q^{1/2} - q^{-1/2}} \tag{2.19}$$

Details of $SU(2)_q - 6j$ symbols can be found in Appendix 1. The Turaev-Viro partition function for a manifold without boundary is

$$\begin{aligned} Z_{TV} \;=\; & \sum_{colourings\; j_e \leq \frac{k}{2}} \; \prod_{vertices} \frac{1}{\Lambda_q} \prod_{e:\; edges} (-1)^{2j_e}[2j_e + 1]_q \;\; \times \\ & \prod_{t:\; tetrahedra} \exp\left(-i\pi \sum_i j_i(t)\right) \begin{Bmatrix} j_1(t) & j_2(t) & j_3(t) \\ j_4(t) & j_5(t) & j_6(t) \end{Bmatrix}_q \end{aligned} \tag{2.20}$$

Here, vertices, edges and tetrahedra are those associated with the triangulation. The subscript q and square brackets indicate q numbers instead of ordinary numbers, and $SU(2)_q - 6j$ symbols instead of ordinary $6j$ symbols. $\Lambda_q = \frac{-2(k+2)}{(q^{1/2} - q^{-1/2})^2}$.

The Turaev-Viro partition function is related to three-dimensional gravity with a cosmological constant where the deformation parameter q is related to the cosmological constant. The $q-6j$ symbol for large j has been shown to be related to the Regge action for a tetrahedron for the case of gravity with a cosmological constant [27]. It has also been shown that the Turaev-Viro partition function is the square of the partition function of SU(2) Chern-Simons theory, where the coupling constant k, is related to the deformation parameter q as $q = \exp\frac{2\pi i}{k+2}$ [28]. The Turaev-Viro partition function, written in terms of Chern-Simons theory is related to the Einstein-Hilbert action for Euclidean gravity as follows: The partition function of the q-analogue lattice model given by the square of SU(2) Chern-Simons partition function, may be rewritten in terms of SL(2, C) Chern-Simons theory as

$$Z_k \;=\; \int [dA,\, d\bar{A}]\, \exp[\frac{ik}{4\pi}\int (AdA + \frac{2}{3}A^3) \;-\; (\bar{A}d\bar{A} + \frac{2}{3}\bar{A}^3\,)] \tag{2.21}$$

where A is an SL(2, C) connection. To relate this to $3-d$ gravity, in terms of the triad e and spin connection field ω, we define $A = \omega + \frac{ie}{l}$ and $\bar{A} = \omega - \frac{ie}{l}$, and denote $I[A] = \frac{k}{4\pi}\int(AdA + \frac{2}{3}A^3)$. Then, the action in (2.21) can be written as the Einstein-Hilbert action of gravity with negative cosmological constant.

$$i(I[A] - I[\bar{A}]) = \frac{1}{16\pi G}\int_M \sqrt{g}(R + \frac{2}{l^2}) = I_{EH} \qquad (2.22)$$

The cosmological constant is $\Lambda = -\frac{1}{l^2}$ and the coupling constant k given by $k = \frac{l}{4G}$.

The issue of writing the Turaev-Viro partition function for a manifold with boundary is tricky. In the picture of Turaev and Viro, one can consider a Heegard splitting of a closed manifold M into two manifolds (handlebodies) M_1 and M_2 with boundary, such that both M_1 and M_2 have the same boundary topology. The Turaev-Viro partition function for M is given by (2.20). Now, M can be obtained by gluing the boundaries of M_1 and M_2 after an appropriate diffeomorphism. Therefore, in this scheme, the partition function for a manifold with boundary should be such that the gluing of two such manifolds yields the correct expression (2.20) for the resulting closed manifold.

For a manifold with boundary, in the expression in (2.20), in addition, there is a factor of $\frac{1}{\sqrt{\Lambda_q}}$ per boundary vertex, and $\exp(i\pi j_b)\sqrt{[2j_b+1]_q}$ per boundary edge with a spin j_b. As mentioned earlier, Z_{TV} is related to $|Z_{SU(2)}|^2$ which is related to Z_{grav}, the partition function of Euclidean gravity. However, as pointed out in [29], the integration measure in the Chern-Simons partition function is $[dA, d\bar{A}]$, whereas for the gravity partition function, it is $[de, d\omega]$. Since $A = \omega + \frac{ie}{l}$, the relation between the two involves $\frac{1}{l}$ factors. It was argued in [29] that for a closed manifold, the factors of $\frac{1}{\Lambda_q}$ appearing in (2.20) are to do precisely with the difference in the measures. This can also be extended to the case of a manifold with boundary, because the choice of $\frac{1}{\sqrt{\Lambda_q}}$ per boundary vertex in the Turaev-Viro partition function was made so that on fusing two such manifolds to make a closed manifold, one obtained the partition function (2.20) for a closed manifold. Therefore, the Turaev-Viro partition function could be thought of as equivalent to the square of a Chern-Simons partition function, but would be equal to a gravity partition function only without the Λ_q terms in (2.20). The partition function for gravity for a manifold with boundary would be given by

$$Z_{grav} = \sum_{colourings\ j_e \leq \frac{k}{2}} \prod_{e:\ internaledges} (-1)^{2j_e}[2j_e+1]_q \times \prod_{b:\ boundaryedges} \exp(i\pi j_b)\sqrt{[2j_b+1]} \times \prod_{t:\ tetrahedra} \exp(-i\pi \sum_i j_i(t)) \left\{ \begin{matrix} j_1(t) & j_2(t) & j_3(t) \\ j_4(t) & j_5(t) & j_6(t) \end{matrix} \right\}_q \tag{2.23}$$

The expression in (2.23) is a functional of the triangulation and spins on the boundary.

It must be pointed out here that this is not the only generalisation of the Turaev-Viro partition function for a manifold with boundary. Recently, another possible generalisation has been proposed in [30] where the partition function is invariant under piece-wise linear homeomorphisms of the triangulation of the manifold. We comment on this generalisation and its possible applications in the concluding chapter.

2.4 The BTZ black hole in the PRTV picture

We would like to compute the entropy associated with the BTZ black hole, and obtain a picture of the states associated with it in the PRTV lattice gravity formalism. The question to be addressed is what the black hole corresponds to in this framework. We recall from section 2 that the Euclidean black hole has a solid torus topology. The horizon is a circle at the core of radius r_+. $|r_-|$ is the amount of twist made before making discrete identifications to obtain the solid torus.

Each triangulation of a solid torus is a realisation of the black hole topology in the lattice picture. With each such triangulation with specified lengths on the boundary is associated a 'partition function' (2.23) which is the contribution corresponding to a fixed boundary metric given by the boundary lengths. The total black hole partition function is formally a path integral over both bulk and boundary metrics - in this case, a sum over spin assignments in the bulk and on the boundary such that the longitude has length $2\pi r_+$. Summing over the spins in the bulk yields an expression of the form (2.23) which is a functional of the spins on the boundary. Summing over the all boundary spins consistent with the circumference being $2\pi r_+$ would give the black hole partition function. We now proceed to estimate the contributions to this sum.

We look at all possible triangulations of this solid torus with different spins on the boundary. Remembering that a spin j corresponds to a length $(\sqrt{j(j+1)})$ in the triangulation , we see that for any given triangulation, the spins will be constrained by the lengths of the circumferences of this solid torus.

We can have an arbitrary triangulation of the solid torus in three steps as follows : In Fig. 4, the torus is formed out of blocks, each of which has two N-polygonal faces of the type in Fig. 5, that are joined to the faces of the next block. Each of these faces can be triangulated, and corresponding triangles on the opposite face can be joined to these triangles, as in Fig. 5, resulting in each block being broken up into a certain number of prisms (six in the case drawn here).

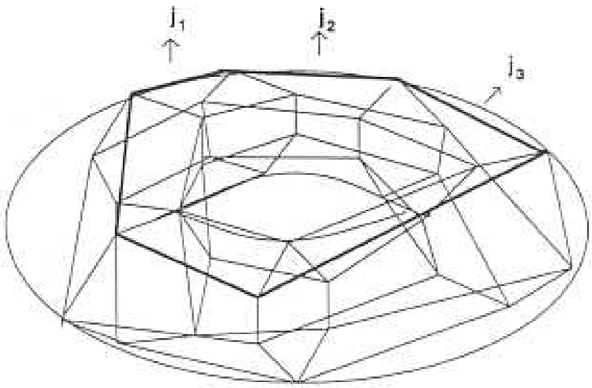

Figure 4. *Torus formed out of polygonal blocks*

Then each prism can be triangulated into tetrahedra, as shown in Fig. 6. These three steps yield a a triangulation of the solid torus. For this triangulation to represent a state of the black hole, however, some of the spins corresponding to the longitudinal cycle must be restricted by the fact that the sum of the lengths associated with them is $2\pi r_+$.

In Fig. 4, we see that the spins j_1, j_2 etc. corresponding to the longitudinal cycle have to satisfy

$$\gamma\ l_p \sum_{i=no.\ of\ blocks} (\sqrt{j(j+1)}) = 2\pi r_+ \qquad (2.24)$$

where the unit of length used is $\gamma\ l_p$. l_p is the Planck length in three dimensions and γ is an arbitrary parameter. There is an ambiguity in the unit of length in the Ponzano-Regge formalism itself. The result of a loop gravity calculation by Rovelli [31] suggests that in Ponzano Regge gravity, the unit of length associated with a spin is l_p. In $(3+1)-d$ canonical gravity [32], [33], there is an arbitrary parameter associated with scaling of the canonical variables, and multiplies the expression for area and volume eigenvalues. Here too, we find that there is an arbitrary parameter γ which multiplies the unit of length l_p obtained in [31], and is associated with scaling of e and ω.

We first consider the case of the torus formed out of blocks of prisms, each of which is triangulated as in Fig. 6. Then, the spins that are restricted in each prism by constraints of the form (2.24) are the longitudinal spins j_{AD}, j_{BE} and j_{CF} and their corresponding counterparts in other prisms

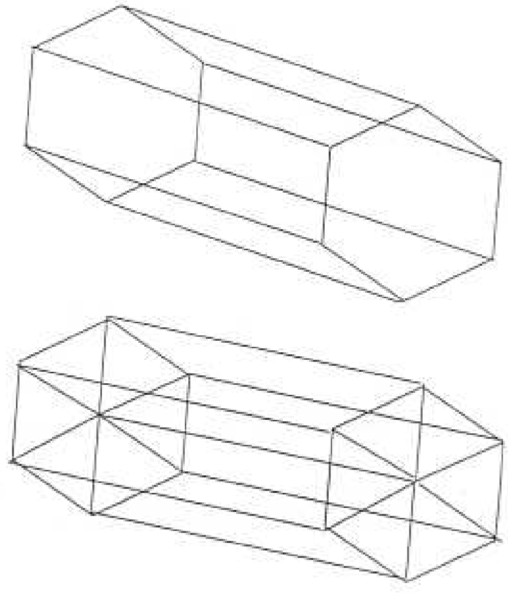

Figure 5. *Polygonal block broken up into prisms*

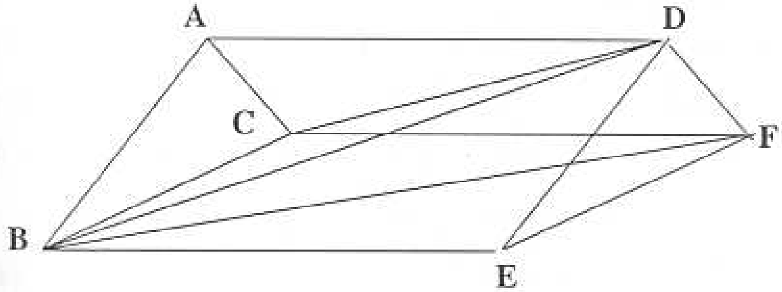

Figure 6. *Triangulation of prism into tetrahedra*

- the length associated with each of these spins when summed with lengths associated with corresponding spins in all other prisms must give $2\pi r_+$.

Given this restriction, we try to estimate the partition function contribution from these prisms for all possible values of the various spins. The contribution can be estimated by considering each prism separately, and then multiplying contributions from all prisms. The contribution of each prism with a certain assignment of spins is given from (2.23) as

$$
\begin{aligned}
Z_b = & \prod_{u:\, unsharededges} \sqrt{[2j_u+1]}\ \exp(i\pi j_u) \prod_{s:\, sharededges} [2j_s+1]^{\frac{1}{4}}\ \exp(\frac{i\pi j_s}{2}) \times \\
& \exp(-i\pi(j_{AB}+j_{AC}+j_{BC}+j_{CD}+j_{AD}+j_{BD})) \begin{Bmatrix} j_{AB} & j_{BC} & j_{AC} \\ j_{CD} & j_{AD} & j_{BD} \end{Bmatrix}_q \times \\
& \exp(-i\pi(j_{BC}+j_{CF}+j_{BF}+j_{DF}+j_{BD}+j_{CD})) \begin{Bmatrix} j_{BC} & j_{CF} & j_{BF} \\ j_{DF} & j_{BD} & j_{CD} \end{Bmatrix}_q \times \\
& \exp(-i\pi(j_{BE}+j_{EF}+j_{BF}+j_{DF}+j_{BD}+j_{ED})) \begin{Bmatrix} j_{BE} & j_{EF} & j_{BF} \\ j_{DF} & j_{BD} & j_{ED} \end{Bmatrix}_q
\end{aligned} \tag{2.25}
$$

Here, j_u refers to the unshared sides and j_s to the sides shared with the blocks to which the prism is fused to form the solid torus.

The expression Z_b corresponds to one prism. For a triangulation with n identical prisms, the contribution would simply be $(Z_b)^n$. It is difficult to calculate the partition function exactly for arbitrary spins associated with the edges. We shall calculate the contribution to the partition function for some specific assignment of spins to argue that dominant contribution comes from a specific assignment below.

The simplest choice of spins we can take is $j_{AB} = j_{AC} = j_{BC} = j_{DE} = j_{EF} = j_{DF} = 0$. Then, the choice of the other spins decides the number of prisms in the triangulation. All the other spins have to be equal, i.e $j_{AD} = j_{CF} = j_{BE} = j_{CD} = j_{BD} = j_{BF} = j$. Geometrically, this corresponds to each prism having collapsed into a line with spin j. Thus, the torus itself collapses to just the longitudinal cycle. Then, from the constraint (2.24), the number of blocks n for fixed r_+ is given by

$$n = \frac{2\pi r_+}{\gamma\, l_p\, \sqrt{j(j+1)}} \tag{2.26}$$

The largest value of n corresponds to the lowest spin, $j = 1/2$. This in turn yields the maximum contribution to the partition function. Each prism contributes a value $[2]_q$, and therefore, the total contribution to the partition function for large k is 2^n, where $n = \frac{4\pi r_+}{\gamma\, l_p\, \sqrt{3}}$.

Any other assignment of spins yields a contribution less than that of this case. To see this, let us consider the case $j_{AB} = j_{AC} = j_{BC} = j_{DE} = j_{EF} = j_{DF} = R$, $(R\ \ large)$, we can take recourse to the following asymptotic formula for the $6j$ symbol for $R \gg 1$ (details in Appendix 1) valid in our case for large k:

$$\left\{ \begin{array}{ccc} a & b & c \\ R & R & R \end{array} \right\} = \frac{(-1)^c}{\sqrt{2R(2c+1)}} C^{c0}_{a0b0} \tag{2.27}$$

where C^{c0}_{a0b0} is the Clebsch-Gordon coefficient.

Here, we find that the largest contribution to the partition function comes again when $j_{AD} = j_{CF} = j_{BE} = 1/2$ and $j_{CD} = j_{BF} = j_{BD} \sim R$. This contribution for large k is $(\sqrt{2})^n$ where n is given by (2.26), and is smaller than the earlier mentioned contribution.

The contribution from the intermediate values of spins remain to be found. The difficulty with calculating this contribution is due to the fact that the $6j$ symbols in the contribution have to be evaluated. In order to obtain this contribution, we look at the corrections to the asymptotic formula (2.27) for R not very large. We find that for $R \geq 2$, considering the corrections, we have

$$\left\{ \begin{array}{ccc} a & b & c \\ R & R & R \end{array} \right\} \leq \frac{(-1)^c}{\sqrt{2R(2c+1)}} C^{c0}_{a0b0} \tag{2.28}$$

We now take the following choice of spins : $j_{AB} = j_{BC} = j_{DE} = j_{EF} = j_{CD} = R$, $j_{AC} = j_{DF} = j_{BD} = j_{BF} = R - j$, $j_{AD} = j_{CF} = j_{BE} = j$.

The contribution of this choice of spins can be estimated using the r.h.s of (2.28). This can be done in two regimes :

i)$R \gg j$. In this case, $R \geq 2$.

ii) $j \gg R$. Here, $j \geq 2$.

Case ii) is estimated numerically. It is found that case i) has a higher contribution, and its contribution is highest for $j = 1/2$. Further, this contribution is less than $(\sqrt{2})^n$. Case i) and ii) describe those values of spins where some spins are larger than others. There are other choices which can be investigated, e.g those where all the spins have the same value. If this is a large value (≥ 2), again it is seen that this contribution is much lesser than $(\sqrt{2})^n$.

Finally, there remains the case where all spins are small. Here, it is possible to do exact calculations for a large number of cases. In all these cases, it is explicitly found that the contribution is less than $(\sqrt{2})^n$. Some examples are :

a)$j_{AB} = j_{BC} = j_{ED} = j_{EF} = j_{AD} = j_{CD} = j_{CF} = j_{BE} = 1/2$,

$j_{AC} = j_{DF} = j_{BF} = j_{BD} = 1$.

This contributes $(4/5)^n$.

b)$j_{AB} = j_{AC} = j_{DE} = j_{DF} = j_{AD} = j_{CF} = j_{BE} = 1/2$,

$j_{BC} = j_{EF} = j_{BD} = j_{CD} = 1, \quad j_{BF} = 3/2$.

This contributes $(\sqrt{32/27})^n$.

c)$j_{AB} = j_{AC} = j_{BC} = j_{DE} = j_{DF} = j_{EF} = 1$,

$j_{AD} = j_{CF} = j_{BE} = 1/2, \quad j_{CD} = j_{BD} = j_{BF} = 3/2$.

This contributes $(\sqrt{50/27})^n$.

Summing the contributions from the prism triangulation from all these different regimes of spin values, we see that the maximum contribution seems to come from the first case considered, where $j_{AB} = j_{AC} = j_{BC} = j_{DE} = j_{EF} = j_{EF} = j_{DF} = 0$ and $j_{AD} = j_{CF} = j_{BE} = j_{CD} = j_{BD} = j_{BF} =$

1/2, and where the torus collapses into the longitudinal cycle.

We have considered upto now, only the prism triangulation of the torus. As mentioned before, the torus can be triangulated by other polygonal blocks, each of which can be triangulated by breaking the block into prisms and triangulating them. Therefore, many of the simplifying methods used here can also be used to determine the contribution from other polygons. For polygonal blocks with large spins on the polygonal sides, it is possible to estimate the contribution, which is less than $(\sqrt{2})^n$. Also, for some simple polygons (cube, pentagon) with very small values of spins on their polygonal sides, it is possible to explicitly calculate the contribution, again less than $(\sqrt{2})^n$.

The discussion above suggests that the maximum contribution on considering *all* possible triangulations would still come from the term corresponding to the torus collapsing to the longitudinal cycle, i.e *from states at the horizon*. This contribution is $([2]_q)^n$, which for large k is simply 2^n.

We note here that r_- does not appear in the calculation of the partition function contributions. This is because it only represents a twist in the solid torus and does not change the contribution of states associated with a triangulation. The untwisted triangulation that we have considered corresponds to a black hole with angular momentum $J = 0$. However, the same contribution would also come from a twisted triangulation which corresponds to another black hole with $J \neq 0$ that has the same value of r_+. Thus, this contribution is the same for all black holes with horizon radius r_+.

Looking at states at a fixed value of r_+ corresponds to working in the microcanonical ensemble. The entropy is therefore given by the logarithm of the partition function. As mentioned above, the leading contribution to the partition function for large k is 2^n. The entropy is then be mainly due to this term, and $S = n\, ln2$. Since $n = \frac{4\pi r_+}{\gamma\, l_p\, \sqrt{3}}$,

$$S = \frac{2\pi r_+}{\gamma\, 4\pi G\, \sqrt{3}}\, ln2 \qquad (2.29)$$

where $2\pi r_+$ is the length of the horizon.

This expression for entropy has factors similar to that obtained in a different context for the Schwarzschild black hole in $(3+1)-d$ in the framework of loop gravity [12], [13]. As mentioned before, in the loop gravity result, there is an arbitrary parameter in the expression for entropy, which is related to scaling of the canonical variables. This is chosen to have a particular value so that the expression for the entropy matches the Bekenstein-Hawking result. On choosing the *same* value, $\frac{ln2}{\pi\sqrt{3}}$, for γ in our expression (2.29) for the entropy, the entropy assumes the familiar form

$$S = \frac{A}{4G} \tag{2.30}$$

where A is the 'area' of the horizon, $2\pi r_+$.

Chapter 3

Partition function for the Euclidean BTZ black hole

We have already analyzed the geometry of the Euclidean BTZ black hole in the previous chapter. Now, we describe in detail, the Chern-Simons formulation of three-dimensional gravity [25, 26]. We use it to compute an exact expression for the partition function of the BTZ black hole. From the partition function, we show that for a black hole with large horizon area, the semi-classical entropy formula is reproduced. The correction to the Bekenstein-Hawking entropy is $-3/2\ \log(area)$. This is in agreement with the entropy correction for the Schwarzschild black hole [7] in the four dimensional canonical gravity formalism [12, 13]; and also with a Lorenzian computation of BTZ black hole entropy [11]. We show that the right expression for the logarithmic correction in the context of the BTZ black hole comes from the modular invariance associated with the toroidal boundary of the black hole.

3.1 (2+1)$-d$ gravity as a Chern-Simons theory

We know that gravity in $(2+1)$ dimensions is simple. The action for pure gravity with a cosmological constant Λ is

$$I = \frac{1}{16\pi G}\int_M d^3x\sqrt{-g}(R-2\Lambda) \tag{3.1}$$

The vacuum Einstein field equation

$$R_{\mu\nu} - \frac{1}{2}g_{\mu\nu}R + \Lambda g_{\mu\nu} = 0 \tag{3.2}$$

In $(2+1)$ dimensions, every solution of (3.2) has a constant curvature, positive if Λ is positive, and negative for Λ negative.

In fact, it is also possible to rewrite gravity as a gauge theory - infinitesimal diffeomorphisms can be regarded as field dependent gauge transformations. Large diffeomorphisms must be handled separately. It was shown by Achucarro and Townsend [25] that this gauge theory is actually a Chern-Simons theory - the action for gravity in the first order formalism can be rewritten as a Chern-Simons action.

The gravity action can be written in the first order formalism in terms of the triad e^a_μ and a spin connection ω^a_μ. The action is

$$I = \int_M \epsilon^{\mu\nu\lambda}(e_{\mu a}(\partial_\nu\omega^a_\lambda - \partial_\lambda\omega^a_\nu) + \epsilon_{abc}e^a_\mu\omega^b_\nu\omega^c_\lambda + \frac{\Lambda}{3}\epsilon_{abc}e^a_\mu e^b_\nu e^c_\lambda) \tag{3.3}$$

For the case of gravity with a negative cosmological constant, we can write this action as a gauge theory for the group $SO(2,2)$. The algebra obeyed by the generators is

$$[J_a, J_b] = \epsilon_{abc}J_c,\ [J_a, P_b] = \epsilon_{abc}P_c,\ [P_a, P_b] = \Lambda\epsilon_{abc}J^c \tag{3.4}$$

We now define a gauge field $A_\mu = e^a_\mu P_a + \omega^a_\mu J_a$. Now, $e^a = e^a_\mu dx^\mu$ and $\omega^a = \frac{1}{2}\epsilon^{abc}\omega_{\mu bc}dx^\mu$. Considering a general gauge transformation with infinitesimal gauge parameter, $u = \rho^a P_a + \tau^a J_a$, the variation of A is

$$\delta A_\mu = -\partial_\mu u - [A_\mu, u] \tag{3.5}$$

The gauge transformation leads to a variation in e^a_μ and ω^a_μ of the form

$$\begin{aligned} \delta e^a_\mu &= -\partial_\mu \rho^a - \epsilon^{abc} e_{\mu b} \tau_c - \epsilon^{abc} \omega_{\mu b} \tau_c \\ \delta \omega^a_\mu &= -\partial_\mu \tau^a - \epsilon^{abc} \omega_{\mu b} \tau_c - \Lambda \epsilon^{abc} e_{\mu b} \rho_c \end{aligned} \tag{3.6}$$

For the particular case of a class of field dependent gauge transformations, i.e for $\rho_a = v^\mu e^a_\mu$ and $\tau^a = v^\mu \omega^a_\mu$, (3.6) reduces to the standard transformation law of the triad and spin connection under diffeomorphisms.

Defining $J^\pm_a = \frac{1}{2}(J_a \pm \frac{1}{\sqrt{\Lambda}} P_a)$, the corresponding connections are $A^a_\mu = \omega^a_\mu \pm \sqrt{\Lambda} e^a_\mu$. Each of the $A^\pm$ can be thought of as an SL$(2,R)$ connection, as SO$(2,2) \simeq$ SL$(2,R) \times$ SL$(2,R)$. Then the first order gravity action can be written as a difference of two Chern-Simons actions,

$$I_{grav} = I_{\rm CS}[A^{(+)}] - I_{\rm CS}[A^{(-)}] \tag{3.7}$$

where the Chern-Simons action $I_{\rm CS}[A]$ is

$$I_{\rm CS} \;=\; \frac{k}{4\pi} \int_M \mathrm{Tr} \left(A \wedge dA + \frac{2}{3} A \wedge A \wedge A \right) \tag{3.8}$$

The Chern-Simons coupling constant $k = -l/4G$.

Euclidean gravity with a negative cosmological constant can be again written as the difference of two Chern-Simons actions as in (3.7), but the gauge group is now SL$(2,\mathbf{C})$. The action for Euclidean gravity is

$$I_{\rm egrav} \;=\; I_{\rm CS}[A] \;-\; I_{\rm CS}[\bar{A}], \tag{3.9}$$

where

$$A \;=\; \left(\omega^a + \frac{i}{l}\, e^a \right) T_a, \qquad \bar{A} \;=\; \left(\omega^a - \frac{i}{l}\, e^a \right) T_a \tag{3.10}$$

are SL$(2,\mathbf{C})$ gauge fields (with $T_a = -i\sigma_a/2$). Here, the negative cosmological constant $\Lambda \;=\; -(1/l^2)$. The Chern-Simons coupling constant is now $k = l/4G$. We see that Lorentzian gravity is obtained back from the Euclidean theory by a continuation $G \to -G$.

It is interesting to note that for Chern-Simons field on a manifold with boundary, a Wess-Zumino conformal field theory is naturally induced on the boundary. Under the decomposition

$$A = g^{-1}dg + g^{-1}\tilde{A}g , \tag{3.11}$$

the Chern-Simons action (3.8) becomes [34, 35]

$$I_{\mathrm{CS}}[A] = I_{\mathrm{CS}}[\tilde{A}] + kI^{+}_{\mathrm{WZW}}[g, \tilde{A}_z] , \tag{3.12}$$

where $I^{+}_{\mathrm{WZW}}[g, \tilde{A}_z]$ is the action of a chiral $SU(2)$ Wess-Zumino model on the boundary ∂M,

$$\begin{aligned} I^{+}_{\mathrm{WZW}}[g, \tilde{A}_z] &= \frac{1}{4\pi}\int_{\partial M} \mathrm{Tr}\left(g^{-1}\partial_z g\, g^{-1}\partial_{\bar{z}} g - 2g^{-1}\partial_{\bar{z}} g \tilde{A}_z\right) \\ &+ \frac{1}{12\pi}\int_M \mathrm{Tr}\left(g^{-1}dg\right)^3 . \end{aligned} \tag{3.13}$$

The 'pure gauge' degrees of freedom g are now true dynamical degrees of freedom at the boundary.

3.2 The Euclidean black hole in the Chern-Simons picture

The Euclidean black hole (2.6) was examined in detail in the previous chapter. It has the topology of a solid torus. We saw that on making a coordinate transformation (2.10), the black hole metric reduces to that of hyperbolic space, with global identifications. The global identifications can be conveniently expressed after a further change of coordinates (2.13). The metric is then

$$ds^2 = \frac{l^2}{R^2 \sin^2\chi}\left[dR^2 + R^2 d\chi^2 + R^2\cos^2\chi d\theta^2\right], \tag{3.14}$$

and the global identifications are given by

$$(\ln R,\ \theta,\ \chi)\ \sim\ (\ln R + \frac{2\pi r_+}{l},\ \theta + \frac{2\pi|r_-|}{l},\ \chi). \tag{3.15}$$

Using (3.10), the connection A^a corresponding to the metric (3.14) may be written as:

$$A^1 \ =\ -\csc\chi\ (d\theta - i\frac{dR}{R}), \qquad A^2 \ =\ i\csc\chi\ d\chi,$$
$$A^3 \ =\ i\cot\chi\ (d\theta - i\frac{dR}{R}). \tag{3.16}$$

The Chern-Simons formulation of gravity was used to describe the BTZ black hole first in [36], where for the Lorentzian black hole, the corresponding gauge fields were evaluated.

In order to compute the black hole partition function, we must evaluate the Chern-Simons path integral on a solid torus. This path integral has been discussed in [34, 37, 38, 39]. Through a suitable gauge transformation, the connection is set to a constant value on the toroidal boundary. In terms of coordinates on the toroidal boundary x and y with unit period, we can define $z = (x + \tau y)$ such that

$$\int_A dz \ =\ 1, \qquad \int_B dz \ =\ \tau \tag{3.17}$$

where A is the contractible cycle and B the non-contractible cycle of the solid torus and $\tau = \tau_1 + i\tau_2$ is the modular parameter of the boundary torus. Then, the connection can be written as [37]:

$$A \ =\ \left(\frac{-i\pi\tilde{u}}{\tau_2}\ d\bar{z} + \frac{i\pi u}{\tau_2}\ dz\right) T_3 \tag{3.18}$$

u and $\tilde{u}$ are canonically conjugate fields and obey the canonical commutation relation:

$$[\tilde{u}, u] \ =\ \frac{2\tau_2}{\pi(k+2)} \tag{3.19}$$

They can be related to the black hole parameters by computing the holonomies of A around the contractible and non-contractible cycles of the solid torus. These holonomies have been computed in [22] for the general case of a rotating BTZ black hole solution with a conical singularity (Θ) at the horizon such that the identifications (3.15) characterizing the black hole now generalize to

$$\begin{aligned} (\ln R,\ \theta,\ \chi) &\sim (\ln R,\ \theta + \ \Theta,\ \chi) \\ (\ln R,\ \theta,\ \chi) &\sim (\ln R + \frac{2\pi r_+}{l},\ \theta + \frac{2\pi|r_-|}{l},\ \chi) \end{aligned} \tag{3.20}$$

The former identification corresponds to the A cycle and the latter to the B cycle. Then the trace of the holonomies around the contractible cycle A and non-contractible cycle B are:

$$Tr(H_A) \ = \ 2\cosh(i\Theta), \qquad Tr(H_B) \ = \ 2\cosh\left(\frac{2\pi}{l}(r_+ + i|r_-|)\right) \tag{3.21}$$

For the classical black hole solution, $\Theta \ = \ 2\pi$. From (3.18),

$$A_z \ = \ \frac{-i\pi}{\tau_2}\,\tilde{u}, \qquad A_{\bar{z}} \ = \ \frac{i\pi}{\tau_2}\,u \tag{3.22}$$

where

$$u = \frac{-i}{2\pi}\left(-i\Theta\tau + \frac{2\pi(r_+ + i|r_-|)}{l}\right), \tilde{u} = \frac{-i}{2\pi}\left(-i\Theta\bar{\tau} + \frac{2\pi(r_+ + i|r_-|)}{l}\right) \tag{3.23}$$

We note here that $\tilde{u}$ is the canonical conjugate, but not the complex conjugate of u. This is so because A is a complex SU(2) connection.

3.3 The Black Hole Partition Function

To compute the black hole partition function in the Chern-Simons formulation, we first write the Chern-Simons path integral on a solid torus with a boundary modular parameter τ. For a fixed boundary value of the connection, i.e. a fixed value of u, this path integral is formally equivalent to a state $\psi_0(u, \tau)$ with no Wilson lines in the solid torus. The states corresponding to having closed Wilson lines (along the non-contractible cycle) carrying spin $j/2$ ($j \leq k$) representations in the solid torus are given by [34, 37, 38, 39]:

$$\psi_j(u,\tau) \;=\; \exp\left\{\frac{\pi k}{4\tau_2}u^2\right\}\;\chi_j(u,\tau), \tag{3.24}$$

where χ_j are the Weyl-Kac characters for affine SU(2). The Weyl-Kac characters can be expressed in terms of the well-known Theta functions as

$$\chi_j(u,\tau) \;=\; \frac{\Theta^{(k+2)}_{j+1}(u,\tau,0) \;-\; \Theta^{(k+2)}_{-j-1}(u,\tau,0)}{\Theta^2_1(u,\tau,0) \;-\; \Theta^2_{-1}(u,\tau,0)} \tag{3.25}$$

where Theta functions are given by:

$$\Theta^k_\mu(u,\tau,z) = \exp(-2\pi ikz)\;\sum_{n\in Z}\exp 2\pi ik\left[(n+\frac{\mu}{2k})^2\tau + (n+\frac{\mu}{2k})u\right] \tag{3.26}$$

The black hole partition function is to be constructed from the boundary state $\psi_0(u,\tau)$. To do that, we note the following:

a) We must first choose the appropriate ensemble. Here, we choose the microcanonical ensemble. As has been discussed in [40], the microcanonical ensemble is characterised by fixing the energy of the system $\bar{E}$, angular momentum J and $\bar{A}$, the "area" or size of the thermodynamic container. In our picture, we keep the value of the holonomy around the non-contractible cycle B fixed. This fixes, from (2.8) and (3.21), the parameters M and J at the boundary. M here corresponds to the energy of the system $\bar{E}$. Further, we recollect that the toroidal boundary is characterised by fixing the coordinate χ in (3.14), which from (2.10) is fixing the value of the Schwarzschild radial coordinate r at the boundary. Characterising the boundary by a fixed r is fixing $\bar{A}$.

Thus we have already fixed all the thermodynamic variables corresponding to the microcanonical ensemble. The holonomy around the contractible cycle A is Θ, which has a value 2π for the classical solution. From [22], Θ, the defect angle at the horizon is a variable conjugate to the area. In the ensemble picture [40], the defect angle Θ is then the canonical pressure variable. It is therefore *not* held fixed in the microcanonical ensemble, and we must sum over contributions to the partition function from all values of

Θ. This corresponds to starting with the value of u for the classical solution, i.e. with $\Theta = 2\pi$ in (3.21), and then considering all other shifts of u of the form

$$u \rightarrow u + \alpha\tau \tag{3.27}$$

where α is an arbitrary number. This is implemented by a translation operator of the form

$$T = \exp\left(\alpha\tau\frac{\partial}{\partial u}\right) \tag{3.28}$$

However, this operator is not gauge invariant. The only gauge-invariant way of implementing these translations is through Verlinde operators of the form

$$W_j = \sum_{n\in\Lambda_j} \exp\left(\frac{-n\pi\bar{\tau}u}{\tau_2} + \frac{n\tau}{k+2}\frac{\partial}{\partial u}\right) \tag{3.29}$$

where $\Lambda_j = -j, -j+2, ..., j-2, j$. This means that all possible shifts in u are not allowed, and from considerations of gauge invariance, the only possible shifts are

$$u \rightarrow u + \frac{n\tau}{k+2} \tag{3.30}$$

where n is always an integer taking a maximum value of k. Thus, the only allowed values of Θ are $2\pi(1+\frac{n}{k+2})$. We know that acting on the state with no Wilson lines in the solid torus with the Verlinde operator W_j corresponds to inserting a Wilson line of spin $j/2$ around the non-contractible cycle. Thus, taking into account all states with different shifted values of u as in (3.30) means that we have to take into account all the states in the boundary corresponding to the insertion of such Wilson lines. These are the states $\psi_j(u,\tau)$ given in (3.24).

b) In order to obtain the final partition function, we must integrate over all values of the modular parameter, i.e. over all inequivalent tori with the same holonomy around the non-contractible cycle. The integrand, which is a function of u and τ, must be the square of the partition function of a gauged $SU(2)_k$ Wess-Zumino model corresponding to the two $SU(2)$

Chern-Simons theories. It must be modular invariant – modular invariance corresponds to large diffeomorphisms of the torus, and the partition function must not change under a modular transformation.

The partition function is then of the form

$$Z = \int d\mu(\tau,\bar{\tau}) \left| \sum_{j=0}^{k} a_j(\tau)\, \psi_j(u,\tau) \right|^2 \tag{3.31}$$

where $d\mu(\tau,\bar{\tau})$ is the modular invariant measure, and the integration is over a fundamental domain in the τ plane. Coefficients $a_j(\tau)$ must be chosen such that the integrand is modular invariant. Under an $\mathcal{S}$ modular transformation, $\tau \to -1/\tau$ and $u \to u/\tau$, the $SU(2)_k$ characters transform as

$$\begin{aligned} \chi_j(u,\tau) &\to \exp\left(-2\pi ik\,\frac{u^2}{4\tau}\right) \chi_j\left(\frac{u}{\tau}, \frac{-1}{\tau}\right) \\ &= \exp\left(-2\pi ik\,\frac{u^2}{4\tau}\right) \sum_l S_{jl}\, \chi_l(u,\tau) \end{aligned} \tag{3.32}$$

where matrix S_{jl} given by

$$S_{jl} = \sqrt{\frac{2}{k+2}}\, \sin\left[\frac{\pi(j+1)(l+1)}{k+2}\right], \qquad 0 \le j,\, l \le k \tag{3.33}$$

We note here that this S matrix is orthogonal: $\sum_j S_{lj}\, S_{jp} = \delta_{lp}$.

We are interested in the transformation property of the state $\psi_j(u,\tau)$ under an $\mathcal{S}$ modular transformation. The prefactor in (3.24) transforms into itself under such a transformation apart from an extra piece that exactly cancels the prefactor in (3.32). Thus, under an $\mathcal{S}$ transformation $(\tau \to -1/\tau)$,

$$\psi_j(u,\tau) \to \sum_l S_{jl}\, \psi_l(u,\tau) \tag{3.34}$$

Under a $\mathcal{T}$ modular transformation $(\tau \to \tau + 1)$, $\psi_j(u,\tau)$ picks up a phase,

$$\psi_j(u,\tau) \to \exp(2\pi i m_j)\, \psi_j(u,\tau) \tag{3.35}$$

where $m_j = \frac{(j+1)^2}{2(k+2)} - \frac{1}{4}$. For the integrand in (3.31) to be modular invariant, the coefficient $a_j(\tau)$ must transform under the $\mathcal{S}$ transformation as $a_j(\tau) \to \sum_p a_p(\tau)\, S_{pj}$ and under the $\mathcal{T}$ transformation as

$a_j(\tau) \rightarrow \exp(-2\pi i m_j)a_j(\tau)$. Further, since the integrand must correspond to the square of the partition function of a gauged $SU(2)_k$ Wess-Zumino model, the coefficients $a_j(\tau)$ are just the complex conjugate of $SU(2)_k$ characters corresponding to $u = 0$, i.e $(\psi_j(0,\tau))^*$. The black hole partition function therefore is

$$Z_{bh} = \int d\mu(\tau,\bar{\tau}) \left| \sum_{j=0}^{k} (\psi_j(0,\tau))^* \, \psi_j(u,\tau) \right|^2 \tag{3.36}$$

Finally the modular invariant measure is

$$d\mu(\tau,\bar{\tau}) = \frac{d\tau d\bar{\tau}}{\tau_2^2} \tag{3.37}$$

The expression (3.36) is an *exact* expression for the partition function of the Euclidean black hole. To make a comparison with the semi-classical entropy of the black hole, we evaluate the expression (3.36) for large horizon radius r_+ by the saddle-point method. Substituting from (3.24), (3.25) and (3.26), the saddle point of the integrand occurs when τ_2 is proportional to r_+ and therefore large. But for τ_2 large, the character χ_j is

$$\chi_j(\tau,u) \sim \exp\left[\frac{\pi i\left(\frac{(j+1)^2}{k+2} - \frac{1}{2}\right)}{2}\tau\right] \frac{\sin\pi(j+1)u}{\sin\pi u} \tag{3.38}$$

We now use in (3.36) the form of the character for large τ_2 from (3.38). In the expression for u in (3.21), we replace Θ by its classical value 2π. The computation has been done with positive coupling constant k and at the end, we must perform an analytic continuation to the Lorentzian black hole, by taking $G \rightarrow -G$. It can be checked that after the analytic continuation, it is the spin $j = 0$ in the sum over characters in (3.36) that dominates the partition function.

We obtain the leading behaviour of the partition function (3.36) for large r_+ (and when $|r_-| << r_+$) by first performing the integration over τ_1 in this regime. The τ_2 integration is done by the method of steepest descent. The saddle-point is at $\tau_2 = r_+/l$. Expanding around the saddle-point, by writing $\tau_2 = r_+/l + x$ and then integrating over x, we obtain

$$Z_{bh} = \frac{l^2}{r_+^2} \exp\left(\frac{-2\pi k r_+}{l}\right) \int dx \exp\left[-\frac{\pi k l}{2r_+} x^2\right] \tag{3.39}$$

The integration produces a factor proportional to $\sqrt{r_+}$. The partition function for the Lorentzian black hole of large horizon area $2\pi r_+$ after the analytic continuation $G \to -G$ is then

$$Z_{Lbh} = \frac{l^2}{r_+^2} \sqrt{\frac{8r_+ G}{\pi l^2}} \exp\left(\frac{2\pi r_+}{4G}\right) \tag{3.40}$$

upto a multiplicative constant. The logarithm of this expression yields the black hole entropy for large horizon length r_+:

$$S = \frac{2\pi r_+}{4G} - \frac{3}{2}\log\left(\frac{2\pi r_+}{4G}\right) + \ldots. \tag{3.41}$$

The leading contribution to the black hole entropy is the familiar Bekenstein-Hawking term. The next-order correction to the semi-classical entropy is the logarithm of the black hole area $2\pi r_+$. The coefficient $-3/2$ of this correction is in agreement with that of the logarithmic correction of semi-classical entropy of four dimensional Schwarzschild black hole first observed in ref. [7] in the quantum geometry formulation of gravity. The semi-classical Bekenstein-Hawking entropy for the BTZ black hole was previously studied in the path integral Euclidean formulation in ref. [42], but the logarithmic correction was not seen there. As described above, the right logarithmic correction is obtained by considering the correct modular invariant measure while integrating over all inequivalent tori (as the holonomy around the non-contractible cycle is held fixed).

The calculation presented here should be contrasted with an earlier calculation of partition function of a BTZ black hole coupled to a scalar field [41]. This is a perturbative one-loop calculation which incorporates a specific type of fluctuation, namely a scalar field. For small r_+, this leads to a different coefficient of the the logarithmic correction in the entropy. On the other hand, our calculation is exact; it includes all possible quantum gravity fluctuations. It is therefore not surprising that the results differ.

3.4 The AdS Gas Partition Function

Finally, we make a few remarks on the AdS gas partition function. It is well-known [19] that for four-dimensional AdS-Schwarzschild black holes, there is a phase transition below a certain temperature from the black hole phase to the AdS gas phase. It is not clear if such a phase transition occurs for the BTZ black hole. It has been proposed by Maldacena and Strominger [43] that such a phase transition may take place. They show that the *action* for the AdS gas can be obtained from that of the BTZ black hole by a transformation. For the case of a non-rotating black hole, this transformation has the form $r_+/l \to l/r_+$.

We can perform this transformation to our expression for the partition function for the black hole. This gives us a candidate partition function for the AdS gas. The AdS gas partition function is

$$Z_{AdS}[r_+] = \int d\mu(\tau, \bar{\tau}) \left| \sum_{j=0}^{k} (\psi_j(0,\tau))^* \; \psi_j(u',\tau) \right|^2 \tag{3.42}$$

where $u' = \frac{-i}{2\pi}\left(-i2\pi\tau + \frac{2\pi l}{r_+}\right)$.

The AdS gas partition function can again be evaluated by saddle-point method. Small r_+ leads to a saddle-point with τ_2 large. In this limit of small r_+ (i.e small temperature), the partition function is

$$Z_{AdS}[r_+] = (\frac{r_+}{l})^{\frac{3}{2}} \; \exp\left(\frac{2\pi l^2}{4r_+ G}\right) \tag{3.43}$$

This, at the leading order, agrees with the corresponding semi-classical expression in ref. [43]. It also shows the sub-leading behaviour as a function of r_+.

Chapter 4

Horizon states for AdS black holes

As we saw in the Introduction, various features of fields in the background of AdS black holes can be related, through the AdS/CFT correspondence, to features of strongly coupled gauge theories.

The propagation of various kinds of matter fields in black hole backgrounds has been well studied and yields information about diverse classical and quantum aspects of black hole physics. Detailed analysis of modes of the scalar, spinor and gauge fields in black hole backgrounds can be found for example, in [44]. In particular, for scalar fields, the energies of these modes are given by the square root of the eigenvalues of the spatial part of the Klein-Gordon operator in that background. For static spacetimes with null singularities, it has been argued [45, 46] that the spatial part of the Klein-Gordon operator is essentially self-adjoint. Further, since it is positive and symmetric, one can choose a positive self-adjoint extension such that the eigenvalues are all positive and hence the energies real. However, as we show in this chapter, in the case of many black hole spacetimes, near the null singularity at the horizon, the zero (time-independent) mode of the scalar field has to be handled separately. In particular, the boundary conditions imposed on the zero mode both at the horizon and at infinity are different from those on the other modes with real energies. In fact, we will show that there are an infinite number of boundary conditions, labeled by a $U(1)$ parameter, that lead to one zero mode solution. This solution could be thought of as a 'horizon state' as it is localized at the horizon.

An interesting application of this analysis is to to the the infinite mass limit of the AdS-Schwarzschild black hole [19]. It leads to results that are of relevance in light of the AdS/CFT correspondence. As proposed by Witten [18], the AdS/CFT duality relating supergravity on anti-de Sitter space to a supersymmetric Yang-Mills theory on the boundary can be extended to non-supersymmetric QCD. The AdS background is replaced by an AdS-Schwarzschild black hole background. Gravity on this background surprisingly does reproduce some features of the strong coupling limit of QCD, like the area law behavior of Wilson loops, confinement, and the glueball mass spectrum with a mass gap [18, 47, 48, 49].

The glueball mass spectrum is reproduced by certain time-independent and normalizable modes obtained by solving the dilaton wave equation in the black hole geometry. These modes were numerically computed first in [47, 48]. These modes are "equilibrium modes" for the black hole, i.e. the current vanishes at the horizon, which has been recognised in [49] as the correct boundary condition to be used at the horizon.

It has been argued that "non-equilibrium" modes of the same black hole (with ingoing boundary conditions at the horizon) give the time scale of approach to thermal equilibrium of the boundary Yang-Mills theory. These modes, i.e. the quasi-normal modes of the black hole, have been computed recently [20, 50, 51].

In this chapter, we study the scalar wave equation in the AdS-Schwarzschild background, and show, that written as a Hamiltonian problem, it is not self-adjoint. Self-adjointness and completeness requires inclusion of modes ignored in [47, 48, 49]. These modes are also equilibrium modes of the black hole but are irregular at the horizon [1]. They are also tachyonic. We suggest that these modes are dual in the AdS/CFT sense to modes in QCD_3 signaling the onset of a Savvidy-Nielsen-Olesen-like instability of the vacuum [52, 53, 54, 55].

The organization of the chapter is as follows: In section 1, we briefly describe two kinds of modes that are commonly discussed in related literature, namely the normalizable equilibrium modes, and the non-normalizable quasi-normal modes, to emphasize the differences between them. We also show that for a massless scalar field propagating in Schwarzschild or Reissner-Nordstrom black hole background, the Klein-Gordon operator is self-adjoint. In section 2, we focus on the zero energy mode of the scalar field in these backgrounds, and in the background of the (1+1)-d black hole [56] as well as the BTZ black hole [6]. The equation obeyed by the zero mode has some unusual properties, which we analyze in section 3. In particular, we show that this state is localized at the horizon. In section 4, we apply the results of section 3 to study the zero mode of the massless scalar field in the background of the infinite mass limit of the AdS-Schwarzschild black hole, and argue that the "horizon states" are necessary for completeness. In section 6, we speculate on the interpretation of these irregular modes in the boundary theory, and suggest that they may be related to a Savvidy-Nielsen-Olesen-like instability.

4.1 Modes of the scalar field in black hole background

As mentioned before, the energies of *normalizable* modes of a scalar field in the exterior of a black hole spacetime (i.e. in the region from the outer horizon to infinity) have real energies.

[1]In [48, 49], the existence of irregular modes is mentioned. However, they are not considered.

This can be verified for the Schwarzschild or Reissner-Nordstrom black hole in the exterior. There are no normalizable mode solutions with complex (or pure imaginary) energies. However, this is not true in a region of the black-hole spacetime near a timelike singularity. For the Reissner-Nordstrom spacetime, in the region between the timelike singularity and the inner horizon, the spatial part of the Klein-Gordon operator is not self-adjoint, as also observed by [57], but can be made self-adjoint by a suitable choice of boundary conditions. There exist boundary conditions for which there is a negative eigenvalue for this operator, leading to a mode solution with imaginary energy. However, this solution cannot be extended to the physical region of interest between the outer horizon and infinity.

Other modes of importance in the context of black holes are the quasi-normal modes (see for example, [58, 59]). We mention them here to clearly distinguish them from the modes we are studying in this chapter. For the case of asymptotically flat black holes, these are defined to be purely **ingoing** near the horizon and **outgoing** at infinity. These are not normalizable, but are of interest as their energies are the characteristic frequencies associated with the perturbation of the black hole. These can in general be complex, and decay with time. In the Schwarzschild and Reissner-Nordstrom cases, there are an infinite number of such modes (see [58] for references) which include purely imaginary modes [60]. Recently, quasi-normal modes for the AdS-Schwarzschild black hole have also been studied [51, 21] - an introduction to quasi-normal modes and the computation of these modes is the subject of the next chapter.

An analysis of the spatial part of the Klein-Gordon operator for the AdS-Schwarzschild black hole shows that as expected in [46], the operator is self-adjoint, and all the normalizable modes have real energies. The AdS-Schwarzschild black hole has a metric

$$ds^2 = -F(r)d\tau^2 + F^{-1}(r)dr^2 + r^2 d\Omega^2, \quad \text{where} \tag{4.1}$$

$$F(r) = (1 + r^2/b^2 - r_0^2/r^2). \tag{4.2}$$

Here b is the radius of curvature of the anti-de Sitter space and r_0 is related to the black hole mass,

$$M = \frac{3A_3 r_0^2}{16\pi G_5} \tag{4.3}$$

and A_3 is the area of a unit 3-sphere.

Let us look at a massless scalar field in this background geometry. One can in principle consider a complex scalar field with charge q and mass m, but for simplicity we shall consider only the massless and uncharged field in the black hole background. The action for such a field Φ is

$$\begin{aligned} S &= -\frac{1}{2}\int \sqrt{|g|}g^{ij}(\partial_i\Phi)(\partial_j\Phi)d^5x, \\ &= -\frac{1}{2}\int_{r_+}^{\infty} dr \int dt \int d\Omega \left[r^3\left\{\frac{\dot{\Phi}^2}{F} + F\Phi'^2 + (1/r^2)\Phi L^2\Phi\right\}\right]. \end{aligned} \tag{4.4}$$

The Klein-Gordon equation for the field Φ can be obtained from above. On making the ansatz

$$\Phi = \frac{f(r)}{r^{3/2}}\, Y(angles)\ \exp -(i\omega t), \tag{4.5}$$

the wave functions are defined on the measure dr/F. The Klein-Gordon equation can then be written in terms of the tortoise coordinate r_*, which is defined by $dr_* = dr/F$. It takes the form

$$-\frac{d^2}{dr_*^2}f + V(r_*)f = \omega^2 f, \tag{4.6}$$

with the measure now being dr_*. The potential is positive, vanishes at the horizon $r_* = -\infty$ and diverges at $r = \infty$. This corresponds to a finite r_* and therefore the solutions have to vanish there. Multiplying (4.6) by the complex conjugate of f and integrating over the spacetime from the horizon to infinity, it can be seen that there can be no normalizable solutions that correspond to ω^2 negative or complex. This is in conformity with the fact that the Klein-Gordon operator is self-adjoint.

4.2 Time independent mode in black hole solutions

The positive energy solutions to the Klein-Gordon equation can be analyzed for most black hole solutions by going to the tortoise coordinate r_* mentioned in the previous section. The solutions behave as $f \sim \exp i\omega(t \pm r_*)$ near the horizon and near infinity. The horizon is at $r_* = -\infty$, while the infinity of the Schwarzschild radial coordinate is either at $r_* = \infty$ or at a finite r_*, depending on the black hole considered. The solutions are plane wave normalizable, and have infinitely oscillating phases at the horizon.

The near-horizon analysis of black hole solutions reveals, however, that the time independent ($\omega = 0$) mode of the scalar field has to be handled carefully.

The metric for an asymptotically flat, spherically symmetric, static black hole in 4-D is of the form

$$ds^2 = -F(r)dt^2 + F^{-1}(r)dr^2 + r^2 d\Omega^2 \equiv g_{ij}dx^i dx^j. \tag{4.7}$$

For a Reissner-Nordstrom black hole,

$$\begin{aligned} F(r) &= -\frac{(r-r_+)(r-r_-)}{r^2}, & (4.8)\\ r_\pm &= Ql_P + El_P \pm (2QEl_P^3 + E^2 l_P^4)^2. & (4.9)\end{aligned}$$

Here, l_P is the Planck length and $E = M - Q/l_P$ is the energy above extremality. For a Schwarzschild black hole, $F(r) = (1 - 2M/r)$.

Let us look at a massless scalar field in this background geometry. The action for such a field ϕ is

$$S = -\frac{1}{2}\int \sqrt{|g|}g^{ij}\partial_i\phi\partial_j\phi. \tag{4.10}$$

If we restrict out attention to spherically symmetric configurations, the action looks like

$$S = -\frac{1}{2}\int \left[-(\dot{\phi})^2 + F^2(r)(\phi')^2\right]\frac{dr}{F(r)}dt. \tag{4.11}$$

This immediately allows us to identify the Lagrangian:

$$L = \frac{1}{2}\int \frac{dr}{F(r)}\left[(\dot{\phi})^2 - F(r)^2(\phi')^2\right]. \qquad (4.12)$$

The modes of the scalar field are obtained from the ansatz that the time dependence of ϕ is $\phi \sim \exp(i\omega t)$. We are interested in the time-independent solutions, so we take $\omega = 0$. Then the Klein-Gordon equation for this case is obtained simply by considering the second term in the Lagrangian, and is

$$H = -\frac{1}{F}\frac{d}{dr}\left(F\frac{d}{dr}\right)\psi = 0, \qquad (4.13)$$

where wave functions are defined on $L^2[(0,\infty), r^2 F dr]$. It is more convenient to work with the measure dr rather than $r^2F(r)dr$, so we make a unitary transformation from $L^2[\mathbf{R}^+, F(r)dr]$ to $L^2[\mathbf{R}^+, dr]$ via $U\psi = \sqrt{r^2F(r)}\psi = \chi$. In this new basis, H reads:

$$H = -\frac{d^2\chi}{dr^2} + \left[\frac{(r^2F)''}{2F} - (\frac{(r^2F)'}{2F})^2\right]\chi = 0. \qquad (4.14)$$

On putting the value of F for the black hole in (4.14) and taking the near-horizon limit, we find that both for the non-extremal black holes, (4.14) in the near-horizon limit is

$$\left(-\frac{d^2}{dx^2} - \frac{1}{4x^2}\right)\chi = 0, \qquad (4.15)$$

where $x = (r - r_+)$ is the near-horizon coordinate. r_+ is the horizon. For the extremal Reissner-Nordstrom solution, however, (4.14) reduces near the horizon to

$$-\frac{d^2\chi}{dx^2} = 0. \qquad (4.16)$$

Another situation where we see a similar equation is the near horizon geometry of the one-dimensional black hole discovered by Witten [56]. The metric for this black hole is of the form

$$ds^2 = -\tanh^2(r/R)dt^2 + dr^2. \qquad (4.17)$$

The action for a scalar field propagating in this background is

$$S = -1/2\int \sqrt{|g|}g^{ij}\partial_i\phi\partial_j\phi drdt. \qquad (4.18)$$

The Lagrangian is

$$L = 1/2 \int \tanh(r/R) \left[\frac{\dot{\phi}^2}{\tanh^2(r/R)} - \phi'^2 \right] dr. \tag{4.19}$$

The Klein-Gordon equation for the zero mode can be calculated from the 2nd term, the functions being defined on $L^2[(0,\infty), \tanh(r/R)dr]$:

$$-\frac{1}{\tanh(r/R)} \frac{d}{dr} \left[\tanh(r/R) \frac{d}{dr} \right] \psi = 0. \tag{4.20}$$

Again, we can make a unitary transformation from $L^2[\mathbf{R}^+, \tanh(r/R)dr]$ to $L^2[\mathbf{R}^+, dr]$ via $U\psi = \sqrt{\tanh(r/R)}\psi = \chi$, the equation now is

$$-\frac{d^2\chi}{dr^2} + \frac{1}{R^2} \left[\frac{-1/4}{\tanh^2(r/R)} + \frac{3}{4} \tanh^2(r/R) - \frac{1}{2} \right] \chi = 0. \tag{4.21}$$

For small r, the equation is approximately

$$-\frac{d^2\chi}{dr^2} - \left[\frac{1}{4r^2} + \frac{1}{2R^2} \right] \chi = 0. \tag{4.22}$$

Another black hole that exhibits the same behavior is the BTZ black hole in $(2+1)-D$ gravity [6]. For simplicity, we take $J = 0$. It has a metric given by

$$ds^2 = -N^2 dt^2 + 1/N^2 dr^2 + r^2 d\phi^2, \tag{4.23}$$

where $N^2 = (r^2/l^2 - M)$, $-1/l^2$ is the curvature of AdS space and M is the black hole mass. Here, again, the near horizon Klein- Gordon equation is

$$-\frac{d^2\psi}{dx^2} - \frac{\psi}{4x^2} = 0, \tag{4.24}$$

where $(r - l\sqrt{M}) = x$ is the near-horizon coordinate. In the case of the Schwarzschild, non-extremal and Reissner-Nordstrom equations, the next-order correction is of order $1/(r - r_+)$.

Thus, in all these cases barring the extremal RN black hole, (4.24) is the near-horizon equation for the zero-mode solution. The solutions, both to (4.24) and the extremal case are discussed in the next section. The eigenvalues of the Hamiltonian which is just the l.h.s of (4.24) and of the operator which is the l.h.s of (4.16) are obtained. The solutions of interest are the zero eigenvalue solutions for that Hamiltonian problem. We will see that the self-adjointness analysis of the Hamiltonian H, i.e the l.h.s operator in (4.24) will help us find these solutions.

4.3 Self-Adjointness of the operator H

As has been discussed in Appendix 2, (and see for example [61, 62]), discussion of self-adjointness (or "hermiticity") for an unbounded operator requires us to look at its deficiency indices.

The Hamiltonian H is a special case of a more general Hamiltonian studied extensively in the literature. It is defined on a domain $L^2[\mathrm{R}^+, dx]$ and is of the form

$$H_\alpha = -\frac{d}{dx^2} + \frac{\alpha}{x^2}. \tag{4.25}$$

Classically, the system described by this Hamiltonian is scale invariant (α is a dimensionless constant). However, the quantum analysis of this operator is much more subtle. As was shown by [63, 64], H_α is essentially self- adjoint only for $\alpha > 3/4$. For $\alpha > 3/4$, the domain of the Hamiltonian is

$$\mathcal{D}_0 = \{\psi \in \mathcal{L}^2(dx), \psi(0) = \psi'(0) = 0\} \tag{4.26}$$

For $\alpha \leq 3/4$, this operator is not essentially self-adjoint (and therefore cannot play the role of a Hamiltonian) and so has to be "extended" to another operator. For this case, the deficiency indices are $(1,1)$, and so the self-adjoint extensions are labeled by a $U(1)$ parameter e^{iz}, which labels the domains $\mathcal{D}_z$ of the Hamiltonian H_z. The set $\mathcal{D}_z$ contains all the vectors in $\mathcal{D}_0$, and vectors of the form $\psi_+ + e^{iz}\psi_-$, where

$$\psi_+ = x^{1/2} H_\nu^{(1)}(xe^{i\pi/4}), \tag{4.27}$$

$$\psi_- = x^{1/2} H_\nu^{(2)}(xe^{-i\pi/4}), \tag{4.28}$$

where $\nu = \sqrt{1/4+\alpha}$, and $H_\nu^{(1,2)}$'s are the Hankel functions $J_\nu \pm iN_\nu$. The small x behavior of $\psi_+ + e^{iz}\psi_-$ is

$$\begin{aligned}\psi_+ + e^{iz}\psi_- \sim \frac{ix^{1/2}}{\sin(\pi\nu)}\Bigg[\left(\frac{x}{2}\right)^{\nu}\frac{e^{-3\pi i\nu/4}-e^{iz+3\pi i\nu/4}}{\Gamma(1+\nu)} \\ +\left(\frac{x}{2}\right)^{-\nu}\frac{e^{iz+i\pi\nu/4}-e^{-i\pi\nu/4}}{\Gamma(1-\nu)}\Bigg]. \end{aligned} \tag{4.29}$$

We can now solve the eigenvalue equation for bound states:

$$-\psi'' + \frac{\alpha}{x^2}\psi = -E\psi. \tag{4.30}$$

For $\alpha \geq 3/4$, there are no bound states. More precisely, there are no normalizable solutions to the Schrödinger equation with negative energy. However, for $-1/4 \leq \alpha < 3/4$ there is exactly one bound state of energy E_b, where E_b is

$$E_b = E(\nu, z) = \left[\frac{\sin(z/2+3\pi\nu/4)}{\sin(z/2+\pi\nu/4)}\right]^{1/\nu}, \tag{4.31}$$

and the corresponding eigenfunction is

$$\psi = N(\sqrt{E_b}x)^{1/2}[J_\nu(i\sqrt{E_b}x) - e^{i\pi\nu}J_{-\nu}(i\sqrt{E_b}x)]. \tag{4.32}$$

The existence of bound states seems to be in contradiction with scale invariance, since scale invariance implies that there is no length scale in the problem, whereas the existence of the bound state provides a scale. This tension can be resolved by looking at how scaling is implemented in the quantum theory. The scaling operator is

$$\Lambda = \frac{xp+px}{2}, \tag{4.33}$$

where $p = -id/dx$. It is easily seen that Λ is symmetric on the domain $\mathcal{D}$ of H, and that for $\alpha > 3/4$, Λ leaves invariant the domain of the Hamiltonian. For $\alpha \leq 3/4$,

$$\Lambda\psi = x^{3/2}[\psi_+ + e^{iz}\psi_-]' \tag{4.34}$$

The small x behavior of the function $\Lambda\psi$ is of the form

$$\begin{aligned}\Lambda\psi \simeq \frac{-i\nu x^{1/2}}{\sin\pi\nu}\Bigg[\left(\frac{x}{2}\right)^{\nu}(2e^{i\pi/4}-1)\left(\frac{e^{-3\pi i\nu/4}-e^{i\tilde{z}+3\pi i\nu/4}}{\Gamma(1+\nu)}\right) \\ + \left(\frac{x}{2}\right)^{-\nu}\left(\frac{e^{i\tilde{z}+i\pi\nu/4}-e^{-i\pi\nu/4}}{\Gamma(1-\nu)}\right)\Bigg] + \cdots, \end{aligned} \tag{4.35}$$

where $\tilde{z} = z + \pi/2$. So $\Lambda\psi$ clearly does not leave the domain of the Hamiltonian invariant. Scale invariance is thus anomalously broken, and this breaking occurs precisely when the Hamiltonian admits non-trivial self-adjoint extensions. This also explains the quantum mechanical emergence of a length scale, namely the bound state energy.

We must remark here that there do exist self-adjoint extensions that preserve scale invariance. For example, if $z = -(\pi\nu/2)$, then there is no bound state. From the point of view of the domains, the operator Λ leaves this domain invariant, implying that scaling can be consistently implemented in the quantum theory.

Now that we know about the subtleties about quantum mechanical evolution in $1/x^2$ potential, we can apply these ideas to our case. The potential near the horizon is like $-1/4x^2$ for the problem of interest.

For the $-1/4x^2$ potential, there are infinite number of bound states for a given fixed self-adjoint extension z. These are given by

$$\begin{aligned} \psi_{E_n}(x) &= N_n\sqrt{x}K_0(\sqrt{E_n}x), \quad n \in \mathbf{Z}, && (4.36) \\ E_n &= \exp\left[\frac{\pi}{2}(1-8n)\cot\frac{z}{2}\right], \quad n \in \mathbf{Z}. && (4.37) \end{aligned}$$

These are found by solving (4.30) for $\alpha = -1/4$ and carefully comparing the behavior of the eigenfunctions with the analog of (4.29) which is

$$\psi = e^{-iz/2}(x^{1/2} + ix^{1/2}\ln x) + e^{iz/2}(x^{1/2} - ix^{1/2}\ln x). \qquad (4.38)$$

Returning to the original problem of finding the zero mode solutions, i.e the solutions to (4.24), we see that demanding self-adjointness of the Hamiltonian gives rise to an infinite number of bound states labeled by an integer n. The zero mode solution is obtained from (4.37) in the $n \to \infty$ limit. In particular, the wave function for the solution to (4.24) near the horizon is

$$\psi = N_n x^{1/2}(1 + \ln(\sqrt{E_n}x)). \qquad (4.39)$$

where E_n is given by (4.37) and N_n is an appropriate normalization factor. Then one takes the limit $n \to \infty$. This leads to a solution that is non-zero

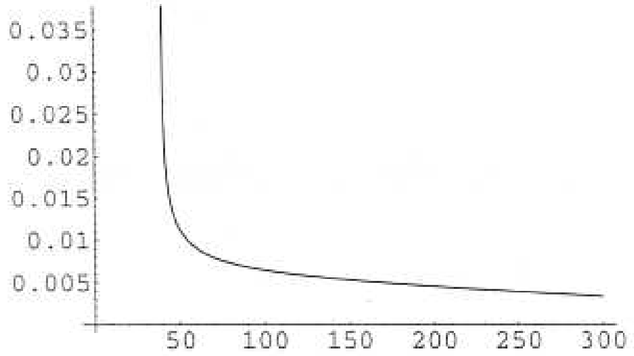

Figure 1.

Absolute value of zero mode solution for a Schwarzschild black hole with horizon radius $r_+ = 50$

only at the horizon, where it peaks, and can be thought of as a 'horizon state'. E_n depends on the self-adjointness parameter z, which also corresponds to the boundary condition at the horizon. However, in the limit $n \to \infty$, all boundary conditions lead to the same solution of (4.24). Since (4.24) is the time-independent zero angular momentum mode for the scalar field in *all* the aforementioned black hole backgrounds, the above discussion applies to all those cases. The behavior of the zero mode found by this method matches that of the numerical zero mode solution for the Schwarzschild black hole in Fig. 1 (where the horizon is at $r = 50$) apart from minor errors in the numerical interpolaion.

For the one exception, the extremal Reissner-Nordstrom black hole, the equation (4.16) is easily solved. The corresponding Hamiltonian problem for which the solutions to (4.16) are the zero eigenvalue solutions was considered in the section above. However, it does not lead to the kind of non-trivial boundary conditions for the zero eigenvalue solution as in the other cases. This is because the self-adjointness analysis of that operator yields only one bound state. The bound state vanishes for a particular value of the self-adjointness parameter, as discussed. Therefore, there seems to be no non-trivial zero mode for the extremal black hole.

4.4 Time-independent modes in the plane AdS black hole

Another black hole solution which can be obtained in the infinite mass limit from the AdS-Schwarzschild solution, the plane AdS solution, was discussed in [18]. The metric for the Euclidean AdS-Schwarzschild black hole in the infinite mass limit is of the form

$$ds^2 = F(r)d\tau^2 + F^{-1}(r)dr^2 + r^2 \sum_{i=1}^{3} dx_i^2, \tag{4.40}$$

where $F(r) = (r^2/b^2 - b^2/r^2)$. Let us look at a massless scalar field in this background geometry. One can in principle consider a complex scalar field with charge q and mass m, but for simplicity we shall consider only the massless and uncharged field in the black hole background. The action for such a field Φ is

$$\begin{aligned} S &= -\frac{1}{2}\int \sqrt{|g|}g^{ij}(\partial_i\Phi)(\partial_j\Phi)d^5x, \qquad (4.41)\\ &= -\frac{1}{2}\int_b^\infty dr \int_0^\beta d\tau \int_{-\infty}^{\infty} d^3x \left[r^3\left\{\frac{\dot{\Phi}^2}{F} + F(\Phi)'^2 + 1/r^2\sum_i(\partial_{x_i}\Phi)^2\right\}\right]. \end{aligned}$$

This action, where the scalar field is the Type IIB dilaton field, has been discussed in [18, 47, 48]. Modes for the field which are τ independent are considered, where $\Phi(r,x) = f(r)\exp(ik.x)$. Then the equation of motion for $f(r)$ is

$$-r^{-1}d/dr(r^3(r^2 - 1/r^2)(df/dr)) + k^2 f = 0, \tag{4.42}$$

where $b = 1$ is taken for simplicity. On demanding normalizability of $f(r)$ w.r.t. the measure r^3dr and regularity of the solution at $r = 1$, a discrete

+5436

negative spectrum for k^2 was obtained. It was identified with the glueball spectrum in the boundary theory.

We show below that one can consider (4.42) as an eigenvalue problem for k^2 and examine the operator in this equation for self-adjointness. As is well known, a self-adjoint operator has only real eigenvalues, and any wave function in the domain of the operator can be written in terms of its eigenfunctions. We therefore wish to find the complete set of k modes such that any function of compact support in the domain can be expanded in terms of the mode functions. It is seen that the operator is not self-adjoint, but can be extended to a self-adjoint operator. However, more general boundary conditions are required at $r = 1$. Then, the spectrum of k is also enlarged to include a discrete infinity of positive k^2 states, and some negative k^2 states as well.

The operator of interest is

$$T = -r^{-1}d/dr[r^3(r^2 - 1/r^2)d/dr], \tag{4.43}$$

where wave functions are defined on a measure r^3dr.

We can therefore check the operator T for self-adjointness. We first check if it is symmetric, i.e. if $(\psi, T\phi) = (T^*\psi, \phi)$, where $\phi \in D(T)$, and $\psi \in D(T^*)$.

If the operator T is symmetric, it is self-adjoint if $(T^* \pm i)\psi = 0$ has no solutions ψ in $D(T^*)$.

But with this measure, we see that the operator is not even symmetric. We therefore consider the measure rdr which from the action (4.42) is the natural measure to consider if one is interested in looking for the eigenvalue problem for the operator (4.43). However, this measure is not enough to guarantee finiteness of the second term in (4.42). Therefore, we take the domain of functions $D(T)$ to consist of C_∞, square integrable functions with respect to the measure rdr which fall off at least as $1/r^3$ (or faster than that) that are of compact support. (Actually, it is enough if they fall of as $1/r^{2+\delta}$ where $\delta > 0$. For convenience, we take $\delta = 1$, and it does not affect any of the analysis.)

The self-adjointness question is easier to address after a change in coordinates, following [48]. On making the transformations

$$
\begin{aligned}
r^2 &= \cosh x, && (4.44)\\
A(x) &= \sqrt{\sinh(2x)}f(x), && (4.45)
\end{aligned}
$$

the measure becomes $dx/\cosh x$, and (4.42) becomes

$$
-4\cosh x\ d^2/dx^2 A(x) + 4\cosh x A(x) - 4\cosh x A(x)/\sinh(2x)^2 = -k^2 A(x) \quad (4.46)
$$

In these coordinates, the horizon is at $x = 0$. Here, one can define the domain of interest $D(T)$ to consist of C_∞, square integrable functions $A(x)$ with respect to the measure $dx/\cosh x$ and which fall off asymptotically at least as $A(x) \sim \exp(-3x/2)$. Also, they are of compact support, so $A(x=0) = A'(x=0) = 0$. Then it can be shown that the operator on the l.h.s of (4.46) is symmetric, however, the domain of the adjoint T^* is now any normalizable function. Thus, $D(T) \neq D(T^*)$. The operator is not self-adjoint. Also, $(T^* + i)\psi = 0$ and $(T^* - i)\psi = 0$ each have one normalizable solution, as can be verified numerically (see Fig. 2). If for each eigenvalue $\pm i$, there is exactly one normalizable solution, then the deficiency indices of this operator are $(1,1)$ and it is possible to find self-adjoint extensions for it. Therefore, one can look for the self-adjoint extension of this operator. Since a self-adjoint extension involves only a change of boundary condition at $x = 0$, we deal with the near-horizon form of (4.46) for simplicity.

On using the near-horizon (x small) approximation, (4.46) becomes

$$
-(d^2/dx^2)A(x) - \frac{A(x)}{4x^2} = -\frac{(k^2+1)A(x)}{4}. \quad (4.47)
$$

This looks like a Hamiltonian problem for a potential $-\frac{1}{4x^2}$ (which was discussed extensively in the previous section) with the eigenvalue $-(k^2+1)/4$.

The results of the previous section can be applied to the case of (4.47) to find the additional states that arise due to the changed boundary

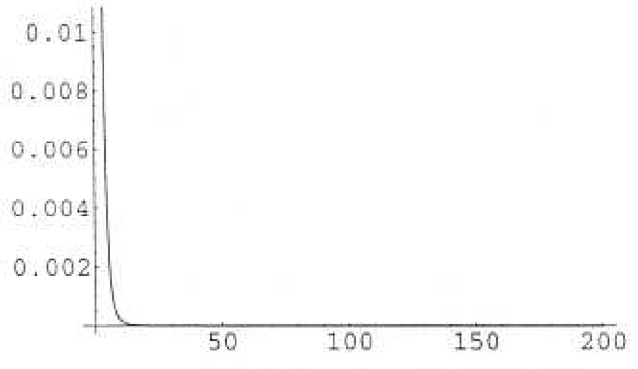

Figure 2.

Absolute value of solution for $k^2 = i$ as a function of r

condition. They are given by (4.37) with $E_n = (k^2+1)/4$. Thus, there are eigenvalues k^2 for each n, and n is any integer. The eigenvalues also depend on the self-adjoint parameter z. There are positive k^2 eigenvalues. There is a possibility of finding some values of k^2 with k^2 negative too, for which $k^2 < 1$.

What has been done above is a near-horizon analysis of (4.46). It is not clear if all of these states are solutions to the complete equation (4.46). However, numerically, there seem to exist normalizable solutions to the complete equation for any positive k^2, provided one also accepts the non-regular solutions that have not been considered by [18, 47, 48]. These are seen to be irregular *only* at the horizon, exactly like the solution in Fig. 2. Imposing a particular boundary condition at the horizon demanded by self-adjointness picks out a discrete infinity of normalizable positive k^2 states as above.

A feature of these modes that is immediately noticeable is that they are irregular at the black hole horizon. However, from considerations of self-adjointness, they are necessary for expressing any arbitrary, *regular* field configuration in the bulk in terms of a complete set of mode solutions. In fact, the difference of any two of these irregular solutions is regular. This is because the irregular solutions are irregular *only* at the horizon, where they behave as $f_k(r) \sim \ln(k(r-1))$ where $r = 1$ is the horizon. Taking the difference of two solutions $f_{k_1}(r)$ and $f_{k_2}(r)$, we see that the resultant solution is regular at the horizon. Therefore, any arbitrary regular field configuration in the bulk can be constructed with regular mode solutions and an even number of irregular mode solutions.

It may seem that the irregular solutions can be gotten rid of by shifting the domain of interest a small distance ϵ away from the horizon, where $\epsilon > 0$ and repeating the self-adjointness analysis for this new domain. However, letting $\epsilon \to 0$, the irregular solutions reappear. Further, the one parameter ambiguity in boundary conditions is not resolved. Letting $\epsilon \to 0$ does not pick any particular boundary condition at the horizon [63].

4.5 Discussion

We find that on examining scalar field theory in the background of the infinite mass limit of the AdS-Schwarzschild black hole, there are more time-independent, *equilibrium* modes than previously obtained [47, 48]. These are however positive k^2 modes. There is a parameter labeling the boundary conditions at the horizon (for the self-adjoint extension) on which these modes depend.

We analyzed the time-independent, $L = 0$ solutions of the $(3+1)-d$ Schwarzschild and Reissner-Nordstrom black holes, the $(1+1)-d$ dilatonic black hole and the BTZ black hole. There are several features in these backgrounds that are similar to the case of the plane AdS-Schwarzschild black hole. In particular, there is again a one parameter family of boundary conditions labeled by the self-adjoint parameter z as before. However, now they lead to the same solution. The solution is a 'horizon state', i.e. it is localized at the horizon. There seems to be no such non-trivial zero mode for the extremal Reissner-Nordstrom black hole.

Lastly, we would like to speculate on the possible interpretation of these irregular modes in the boundary theory. As first observed by [18], the modes with negative k^2 correspond to glueballs with mass k^2. This correspondence, when applied to the irregular states, seem to imply the existence of tachyonic glueball states. Actually, such a scenario is not as exotic as it may appear to be at first sight. It was pointed out a long time ago by Savvidy [52], and also by Nielsen and collaborators [53, 54, 55] that the perturbative vacuum of QCD (when there is a constant colour magnetic field background) is unstable. Considering a translation invariant background for SU(2) gauge fields, they obtained the effective one-loop potential. This has the structure of a double well potential along with an imaginary term signalling the onset of instability. This persists in SU(N) theories and at finite temperature [65]. Our scenario seems to suggest such an instability that perhaps appears due to the choice of the plane-AdS black hole in the bulk, as indicated by the presence of these modes. We comment more on this in the last chapter.

Chapter 5

Quasi-normal modes of AdS black holes

Numerical studies of perturbations of black holes have revealed the presence of certain characteristic modes that govern the time evolution of the initial perturbation. In particular, they dominate the decay of the perturbation at late times. These modes seem to depend only on the black hole parameters and not on the nature of the perturbation. This was first recognised by Vishveshvara [66] while studying perturbations of Schwarzschild black holes. Since then, perturbations of asymptotically flat black holes have been analysed and these characteristic modes(called quasi-normal modes) have been found for some black holes (a detailed account can be found in [59], [58]).

Recently, there has been an interest in quasi-normal modes of AdS black holes in light of the AdS/CFT correspondence [17]. There is some evidence to suggest that an off-equilibrium configuration (like a perturbed black hole or black hole formation from collapse of matter) in the bulk AdS space is related to an off equilibrium state in the boundary theory. A particular example is [67], where black hole formation by collapse of a thin shell in AdS space is investigated. The shell is related by AdS/CFT duality to an off-equilibrium state in the boundary theory which evolves towards equilibrium when the shell collapses to form a black hole.

A quasi-normal mode governs the decay in time of a perturbation of the black hole configuration in the bulk. It should therefore be related by AdS/CFT duality to the return of the boundary Yang-Mills theory to thermal equilibrium. The role of ingoing modes in determining the thermalization time scale of the boundary Yang-Mills theory was pointed out in [50]. A numerical computation of quasi-normal mode frequencies for AdS black holes in various dimensions has been done in [51].

In this chapter, we compute the quasi-normal modes for the AdS-Schwarzschild black hole in five dimensions using a superpotential approach. This is done for the perturbation of a black hole by a minimally coupled scalar field. Time-independent normal modes of a scalar field in the background of this black hole have already been analysed in the last chapter(see also [20, 18]).

We notice, that for the $(2+1)-d$ BTZ black hole, exact quasi-normal mode solutions can be obtained from the Klein-Gordon equation as the black hole potential belongs to a class of exactly solvable potentials, derived from a superpotential.

We propose, based on analogy with the results for the $(2+1)-d$ BTZ black hole, and on numerical evidence in five dimensions, that the black hole potential can be described by a potential series derived from a superpotential. The problem is then exactly solvable and the form of the quasi-normal mode wave function is thus known. This is used as an ansatz to obtain the quasi-normal modes of the AdS_5 black hole. However, the numerical values of the mode frequencies do not agree with the earlier calculation in [51]. We comment on this discrepancy.

The organisation of this chapter is as follows: The next section is a brief review of quasi-normal modes and their properties, and a short summary of some numerical approaches to computing these modes.

The actual computation of quasi-normal(QN) modes for the

AdS_5-Schwarzschild black hole is described in Section 2. First, the QN modes for the $(2+1)-d$ BTZ black hole are evaluated. Motivated by this, a superpotential approach to finding the QN modes for the five-dimensional black hole is presented and the mode frequencies obtained.

In Section 3, we discuss our results. We show that the behaviour of the modes computed numerically by us for small black holes is consistent with that expected from the differential equation obeyed by the mode solutions. We mention salient points of two earlier papers [50] and [51] on the subject and comment on the discrepancy between the numerical values obtained by us and those in [51]. We also state work in progress on QN modes for the RN AdS_5 black hole, and black holes in other dimensions.

5.1 Quasi-normal modes and their properties

Quasi-normal modes of a black hole are characteristic modes associated with the decay of any perturbation outside a black hole. In general, these modes do not form a complete set, in the sense that the decay in time of a perturbation cannot be described *completely* in terms of them. However, they dominate the decay at certain intermediate or late times. To compute these modes, one studies the decay of an initial perturbation by imposing ingoing boundary conditions at the horizon and (for asymptotically flat black holes) outgoing boundary conditions at infinity. This ensures that no gravitational wave from the horizon or infinity disturbs the initial perturbation. Due to these boundary conditions, the quasi-normal modes are complex. The mode wave functions are non-normalisable in space but exponentially decay in time. Since the exact mode wave functions are not known even for the Schwarzschild black hole, there exist only numerical computations of quasi-normal modes. These are also very difficult to do as it is not easy to isolate the purely ingoing wave near the horizon that is also outgoing at infinity. Such a wave function blows up at these points and could be contaminated by a small outgoing part at the horizon or a small ingoing part at infinity where these parts go exponentially to zero. A unique boundary condition to isolate quasi-normal modes has been given by Nollert [59]. The QN modes are poles of the Green's function corresponding to the wave equation obeyed by the perturbing field. Using this, the QN modes for the Schwarzschild and Reissner-Nordstrom black holes were evaluated numerically [44], [68]. WKB methods have also been used to calculate these modes [69] (see also [59] for more references).

The method of continued fractions [70] gives very accurate results for the modes. Here, after removing the singular parts at the horizon and infinity, the QN mode wave function is expanded as a series. The coefficients in the series obey a three-term recurrence relation and depend on the quasi-normal mode frequency. The frequencies then have to satisfy a continued fraction relation. An interesting analytic approach to computing the QN modes is by approximating the black hole potential by an exactly solvable potential (the Poschl-Teller or Eckart potential) [71], [72]. Ferrari and Mashhoon [71] have mapped the problem of QNMs of the Poschl-Teller potential to the bound states of the inverse potential and computed the modes. These approximate the fundamental QN modes of the Schwarzschild black hole well.

For the case of asymptotically anti-deSitter black holes, the black hole potential diverges at infinity. Therefore, as pointed out in [51], the quasi-normal modes are defined to be those that are ingoing at the horizon, but fall off to zero at infinity. It can be shown that this also agrees with the unique boundary condition of Nollert [59] for obtaining quasi-normal modes. However, due to the divergence of the AdS black hole potential at infinity, most of the methods described above to compute the QN modes of asymptotically flat black holes cannot be used directly. It is seen that a combination of two methods, inspired by the case of the $(2+1)-d$ black hole, yields good results.

5.2 Numerical computation of quasi-normal modes

We first consider the case of the QN modes of the non-rotating $(2+1)-d$ BTZ black hole [6]. The non-rotating BTZ black hole metric for a spacetime with negative cosmological constant $\Lambda = -\frac{1}{l^2}$ is given by

$$ds^2 \;=\; -(N)^2\, dt^2 + (N)^{-2}\, dr^2 + r^2\, (d\phi)^2 \tag{5.1}$$

with

$$N \;=\; \sqrt{(-M + \frac{r^2}{l^2})} \tag{5.2}$$

The horizon radius $r_+ = \sqrt{M}l$. We consider a massless scalar field in the black hole background. The Klein-Gordon equation for the scalar field is written using an ansatz for the field

$$\Phi = \frac{1}{\sqrt{r}}\, \chi(r)\, \exp(i\omega\phi) \tag{5.3}$$

and by going to the tortoise coordinate r_* where $dr_* = \frac{dr}{N^2}$. The Klein-Gordon equation is

$$-\frac{d^2\chi}{dr_*^2} + V(r)\chi \;=\; \omega^2\chi \tag{5.4}$$

where

$$V \;=\; \frac{3r^2}{4l^4} - \frac{M}{2l^2} - \frac{M^2}{4r^2} \tag{5.5}$$

Since $r = -r_+ \coth(\alpha r_*)$ where

$$\alpha \;=\; \frac{1}{2}\,\frac{d(N^2)}{dr}(r_+) \;=\; \frac{\sqrt{M}}{l} \tag{5.6}$$

$$V \;=\; \frac{M}{4l^2}\,\left(\frac{3}{(\sinh(\alpha r_*))^2} + \frac{1}{(\cosh(\alpha r_*))^2}\right) \tag{5.7}$$

α is the surface gravity of the black hole and is equal to $2\pi T$ where T is the Hawking temperature.

This potential can be obtained from a superpotential [73] of the form

$$W \;=\; A\,\coth(\alpha r_*) \;+\; B\,\tanh(\alpha r_*) \tag{5.8}$$

by

$$V \;=\; W^2 \;-\; (W)' \;-\; A^2 \;-\; B^2 \;-\; 2AB \tag{5.9}$$

Here, from (5.7),

$$A \;=\; -\alpha(1/2 \pm 1) \tag{5.10}$$

$$B \;=\; -\frac{\alpha}{2} \tag{5.11}$$

As discussed in [73], the lowest energy state for the potential $W^2 - (W)'$ has energy zero, so the lowest energy for the potential V is $-(A+B)^2$. The wave function corresponding to this state is

$$\chi \;=\; \exp(-\int(W)) \;\;=\;\; (\sinh(\alpha r_*))^{-A/\alpha}\;\;(\cosh(\alpha r_*))^{-B/\alpha} \tag{5.12}$$

For any of the two values of A and B in (5.11), the wave function (5.12) is not normalisable. It blows up either at the horizon or at $r = \infty$ (i.e $r_* = 0$). We are interested in the quasi-normal mode solution that blows up at the horizon and falls off to zero at infinity. This corresponds to $A = -(3/2)\alpha$. Also, $B = -\frac{\alpha}{2}$. The lowest energy (formally, since the wave function corresponding to this is non-normalisable) is then

$$E \;=\; -4\alpha^2 \tag{5.13}$$

and the lowest quasi-normal mode $\omega = \sqrt{E}$. Therefore,

$$\omega \;\;=\;\; -2\,i\,\alpha \tag{5.14}$$

Thus, for a given horizon radius $r_+ = \sqrt{M l}$, we can calculate α taking $l = 1$. Then we can read off the value of the lowest quasi-normal mode.

The case of the quasi-normal modes of the AdS_5-Schwarzschild black hole is not so simple as the black hole potential is more complicated than the BTZ case.

The metric for this black hole is

$$ds^2 = -(N)^2\, dt^2 + (N)^{-2}\, dr^2 + r^2\, (d\Omega_3)^2 \tag{5.15}$$

with

$$N = \sqrt{1 + (r/l)^2 - (r_0/r)^2} \tag{5.16}$$

where the black hole mass M is

$$M = \frac{3A_3 r_0^2}{16\pi G_5} \tag{5.17}$$

and A_3 is the area of a unit 3-sphere. The Klein-Gordon equation for the scalar field in the background of this black hole can be written, as before, as a potential problem. Using the ansatz for the field

$$\Phi = \left(\frac{1}{r}\right)^{3/2} \chi(r) Y(angles) \tag{5.18}$$

and by changing to the tortoise coordinate given by $dr_* = \frac{dr}{N^2}$, the Klein Gordon equation is

$$-\frac{d^2\chi}{dr_*^2} + V(r)\,\chi = \omega^2\,\chi \tag{5.19}$$

where

$$V(r) = \left(\frac{15}{4} + \frac{3}{4r^2} + \frac{9r_0^2}{4r^4}\right)\left(1 + r^2 - \frac{r_0^2}{r^2}\right) \tag{5.20}$$

Here, for simplicity, we have taken $l = 1$. If the potential could be written as an exactly solvable potential in the r_* coordinate, then the quasi-normal modes could be obtained easily from the 'lowest' energy, as in the BTZ case. As mentioned in the previous section, the fundamental QN modes of the Schwarzschild black hole were closely approximated by the

QN modes of the Poschl-Teller potential. This is also an exactly solvable potential derivable from a superpotential [73].

We propose that the potential can be written as a series, derived from a superpotential of the form

$$W = \sum_{n=1}^{\infty} A_n \coth(n\alpha r_*) \tag{5.21}$$

where as in (5.6), α is the black hole surface gravity,

$$\alpha = (1/2)\,\frac{d(N^2)}{dr}(r_+) = r_+ + \frac{r_0^2}{r_+^3} \tag{5.22}$$

As before, $\alpha = 2\pi T$, where T is the Hawking temperature.

The potential derived from this series as in (5.9) is

$$V_s = \sum_{n=1}^{\infty} \frac{(A_n^2 + nA_n\alpha)}{\sinh^2(n\alpha r_*)} + \sum_{n,m=1,\ n\neq m}^{\infty} \frac{A_n A_m}{\tanh(n\alpha r_*)\tanh(m\alpha r_*)} \tag{5.23}$$

It has lowest energy

$$E = -(\sum_{n=1}^{\infty} A_n)^2 \tag{5.24}$$

The form of the potential is such that it goes exponentially to zero in r_* as $r \to r_+$ and blows up as $1/r_*^2$ as $r_* \to 0$ (or $r \to \infty$). This reproduces the behaviour of the black hole potential. We propose that this potential series is exactly equal to the black hole potential (5.20). Terminating this potential series at finite order would then mean an approximation to the black hole potential in the spirit of the Poschl-Teller method for asymptotically flat black holes. The wave function corresponding to the lowest energy state is

$$\chi = \exp(-\int(W)) = \prod_{n=1}^{\infty}(\sinh(n\alpha r_*))^{-A_n/(n\alpha)} \tag{5.25}$$

It is non-normalisable, as in the $(2+1)-d$ case. In order to calculate the quasi-normal modes for the AdS-Schwarzschild black hole, we use (5.25) as an ansatz in the equation (5.19). However, we truncate the product in the ansatz upto some finite order. This is equivalent to truncating the potential series. We first write

$$\chi = \psi\,\exp(-i\omega r_*) \tag{5.26}$$

This isolates the non-normalisable part of the wave function. We can rewrite (5.19) as an equation for ψ as

$$-\frac{d^2\psi}{dr_*^2} + 2i\omega\frac{d\psi}{dr_*} + V(r)\psi = 0 \tag{5.27}$$

Here, V is the black hole potential (5.20). We now try to solve for ω by taking the ansatz

$$\psi = \prod_{n=1}^{N}(1 - \exp(2n\alpha r_*))^{-\frac{A_n}{n\alpha}} \tag{5.28}$$

This ansatz is obtained from (5.25) which was an ansatz for χ. Thus, N represents the order upto which V_s has been truncated.

The ansatz for ψ is substituted into (5.27) and the l.h.s of (5.27) is expanded as a series in $(x - x_+)$ where

$$\begin{aligned} x &= \frac{1}{r} \\ x_+ &= \frac{1}{r_+} \end{aligned} \tag{5.29}$$

From (5.27), each term of the series is to be equated to zero. We first divide (5.27) by ψ. Then, we have

$$\begin{aligned} &-4(\sum_{m=1}^{N} A_m K_m)^2 - 4\,\alpha\,(\sum_{m=1}^{N} mA_m K_m) - \\ &4\,\alpha\,(\sum_{m=1}^{N} mA_m K_m^2) + 4\,i\omega\,(\sum_{m=1}^{N} A_m K_m) + V = 0 \end{aligned} \tag{5.30}$$

where

$$K_m = \frac{\exp(2m\alpha r_*)}{1 - \exp((2m\alpha r_*)} \tag{5.31}$$

Expanding each of the terms in the l.h.s of (5.30),

$$K_m = \sum_{n=0} c_m(n)\,(x - x_+)^n \tag{5.32}$$

$$K_m^2 = \sum_{n=0} d_m(n)\,(x - x_+)^n \tag{5.33}$$

$$V = \sum_{n=0} V_n\,(x - x_+)^n \tag{5.34}$$

Substituting these expansions into (5.30), and equating the term of order $(x - x_+)$ in the l.h.s to zero, we obtain

$$A_1 = -\frac{\alpha(\frac{15}{4} + \frac{3x_+^2}{4} + \frac{9r_0^2x_+^4}{4})}{2(i\omega - \alpha)c_1(1)} \tag{5.35}$$

Similarly, equating the term of order $(x - x_+)^N$ in the l.h.s to zero, we obtain a recursion relation for A_N.

$$\begin{aligned} A_N = & \frac{-\alpha(\sum_{m=1}^{N-1} mA_m c_m(N))}{(N\alpha - i\omega)c_N(N)} - \frac{\alpha(\sum_{m=1}^{N-1} mA_m d_m(N))}{(N\alpha - i\omega)c_N(N)} \\ & - \frac{(\sum_{m,n=1}^{N-1} \sum_{N1,N2;N1+N2=N} A_m A_n c_m(N1) c_n(N2))}{(N\alpha - i\omega)c_N(N)} \\ & + i\omega \frac{(\sum_{m=1}^{N-1} A_m c_m(N))}{(N\alpha - i\omega)c_N(N)} + \frac{V_N}{4(N\alpha - i\omega)c_N(N)} \end{aligned} \tag{5.36}$$

The A_n coefficients are functions of ω and of the black hole parameters. The recursion relation for the A_n is complicated, unlike the case of the method of partial fractions [70] applied to asymptotically flat black holes. There, an ansatz was taken for the wave function (removing its singular part) and it was expanded as a series whose coefficients obeyed a simple three-term recursion relation. From (5.27), as $r_* \to 0$ (i.e as $r \to \infty$), the two kinds of solutions are $\psi \sim r_*^{\frac{-3}{2}}$ and $\psi \sim r_*^{\frac{5}{2}}$. The first solution is not normalisable. We want the quasi-normal mode solution to vanish as $r_* \to 0$. So we choose the second solution. But from our ansatz (5.28) for the solution, this implies a relation between the coefficients A_n. More precisely,

$$\sum_{n=1}^{N} \frac{A_n}{n\alpha} = -5/2 \tag{5.37}$$

Since the A_n coefficients are functions of ω, this relation gives the value of the lowest quasi-normal mode as a function of the black hole parameters. This would then be an approximation to the actual QN mode of the black hole at order N. Thus, the asymptotic behaviour of the actual

Radius r_+	Re(ω)	Im(ω)
1	0.6948	1.4648
2	1.0713	1.9817
5	2.4462	4.2642
10	4.8249	8.3279
50	24.0159	41.3183
100	48.0251	82.6165
150	72.0358	123.9190
500	240.1150	413.0500
750	360.1720	619.5740
1000	480.2290	826.0980

Table 1.

solution is *explicitly* demanded of the ansatz. This is *used* to obtain the mode frequencies from the relation (5.37).

We have used this method to calculate the QN modes at various orders N. We find that as we increase N, there is a convergence in the mode frequency. The mode frequencies are given in Table 1. They have been calculated at order $N = 18$. Beyond this order, as (5.37) is complicated, it becomes computationally time-consuming to find its roots. However, as there is a clear convergence in the mode frequency as one increases the order from $N = 1$ and as the percentage difference between the real and imaginary parts of the mode frequency at order $N = 18$ and $N = 17$ is about 1% (for $Re\omega$, it is 1.26%, and for $Im\omega$, it is 1.09%), these numbers should be a good approximation to the QN modes of the black hole (more discussion on results is given in the next section).

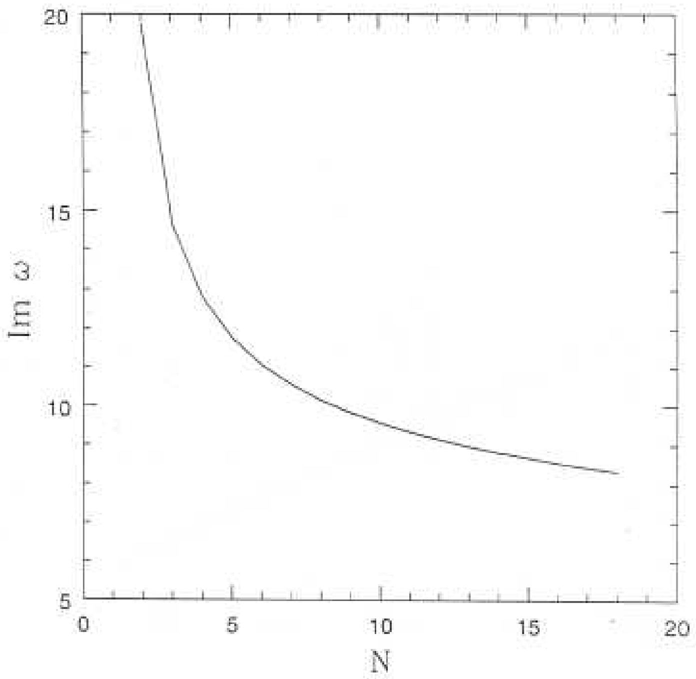

Fig. 1

Figure 1. *Convergence in $Im(\omega)$ as order N is increased, for $r_+ = 10$*

5.3 Discussion of results

The lowest quasi-normal mode frequencies for different horizon radii r_+ are given in Table 1. As mentioned in the last section, there is a convergence in the mode frequency as the order N is increased. The convergence curve for $r_+ = 10$ is given in Fig.1. The rate of convergence does not seem to depend on the value of the horizon radius r_+.

The real and imaginary parts of the mode frequencies are plotted as a function of r_+ for large r_+ in Fig.2a and Fig.2b.

It is seen that the both the imaginary and real parts of the mode frequency are proportional to r_+ for *large* r_+. The real and imaginary

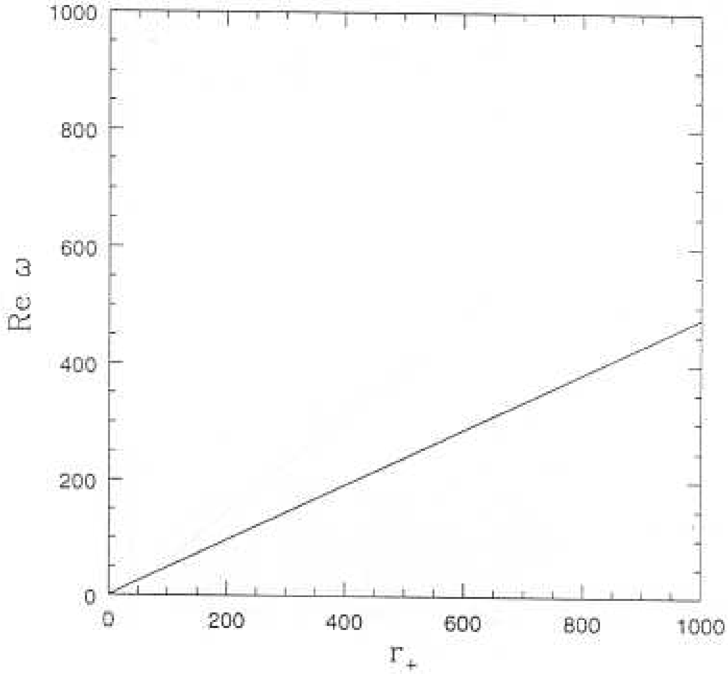

Fig. 2a

Figure 2a. *$Re(\omega)$ as a function of r_+ for large r_+*

parts of the mode frequency can also be plotted as a function of the surface gravity α. It is seen that for *both* small and large r_+, the real and imaginary parts of the frequency are approximately proportional to α. $Re(\omega) \sim 0.24\ \alpha$ and $Im(\omega) \sim 0.41\ \alpha$ provides a good fit for the data. In the case of the QN modes where the modes could be obtained exactly, we saw that they were proportional to the surface gravity. Our numerical results seem to suggest that this may be true even for the five dimensional black hole - at least for very small and very large black holes. The surface gravity $\alpha = (2r_+ + \frac{1}{r_+})$. Therefore, α is large for very small and very large black holes. We have verified numerically that for very small black holes, the mode frequencies are very large, and $\omega \sim \frac{1}{r_+}$. This behaviour of the mode frequency is expected -

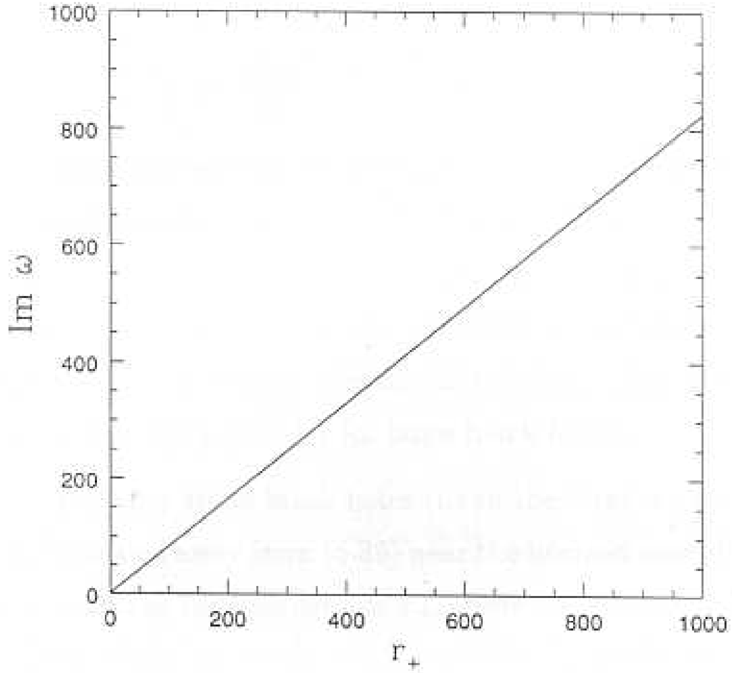

Fig. 2b

Figure 2b. *$Im(\omega)$ as a function of r_+ for large r_+*

as can be seen from the differential equation (5.27) on changing to the inverse radial coordinate x given by (5.29). Then, the differential equation in these coordinates is

$$(-r_0^2 x^6 + x^4 + x^2)\frac{d^2\psi}{dx^2} \; + \; (2x^3 - 4r_0^2 x^5 + 2i\omega x^2)\frac{d\psi}{dx} \; - $$
$$(\frac{15}{4} + \frac{3x^2}{4} + \frac{9r_0^2 x^4}{4})\psi \; = \; 0 \qquad (5.38)$$

Now, we scale x as $x \; = \; q \, x_+$ (where $x_+ = \frac{1}{r_+}$). Now, (5.38) is

$$
\begin{aligned}
(-x_+^2 q^6 - q^6 + x_+^2 q^4 + q^2)\frac{d^2\psi}{dq^2} &+ \\
(2x_+^2 q^3 - 4x_+^2 q^5 - 4q^5 + 2i\omega x_+ q^2)\frac{d\psi}{dq} &- \\
(\frac{15}{4} + \frac{3x_+^2 q^2}{4} + \frac{9x_+^2 q^4}{4} + \frac{9q^4}{4})\psi &= 0 \qquad (5.39)
\end{aligned}
$$

Then we see that for very large black holes (small x_+ approximation), x_+ can be scaled away from (5.39) near the horizon in this approximation provided $\omega = \frac{C}{x_+}$ where C is a constant independent of x_+. It can also be checked that near the horizon, there are no solutions to the scaled equation with $C = 0$, except the trivial solution. This shows that ω is indeed proportional to r_+ (i.e $\frac{1}{x_+}$) for large black holes.

For very small black holes (i.e in the large x_+ approximation), again x_+ can be scaled away from (5.39) near the horizon provided $\omega = D\, x_+$ where D is a constant independent of x_+. Here too, it can be checked that near the horizon, there are no solutions to (5.39) in the large x_+ approximation with $D = 0$ (except the trivial solution). This implies that for small black holes, ω is proportional to $\frac{1}{r_+}$ (i.e to x_+). This is also just a reflection of the fact that a very small AdS-Schwarzschild black hole has negative specific heat and actually resembles a Schwarzschild black hole.

We now examine the previous numerical work on QN modes of AdS black holes in four, five and seven dimensions.

However, the numerical results obtained in [51] for the five dimensional black hole do not agree with our values for the QN modes. There, the solution to (5.27) is expanded as a series around the horizon in the inverse radial coordinate $x = 1/r$. Using this, the l.h.s of (5.27) is expanded as a series around the horizon, and a recursion relation is obtained for the coefficients in the expansion of the solution. The coefficients a_n are functions of the black hole parameters and the mode frequency ω. Therefore,

$$
\psi = \sum_n a_n(\omega)\,(x - x_+)^n \qquad (5.40)
$$

The mode frequencies are then the roots of the equation obtained by setting the series to zero at $x = 0$. In actual computation, the series is truncated,

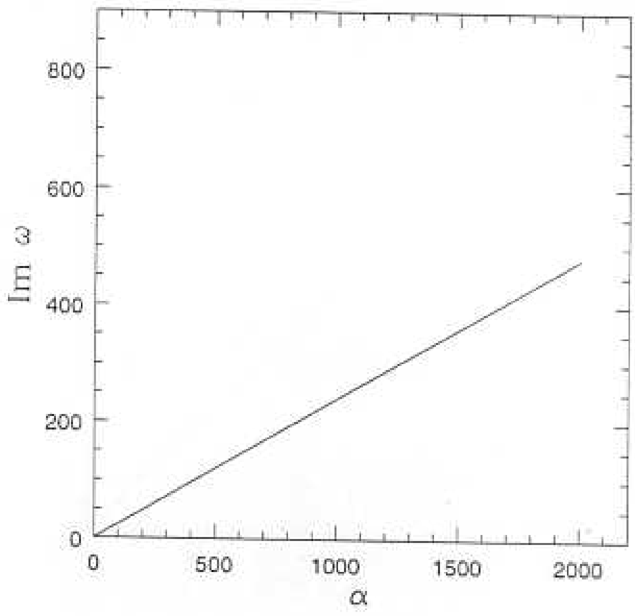

Fig. 3a

Figure 3a. *Re(ω) as a function of α*

and the roots obtained. However, the mode frequencies seem to go to zero as $r_+ \to 0$, which is not the behaviour expected from the differential equation. We also wish to make a comment here on a numerical integration by Zhu et.al [74] where it is claimed that the modes of the five-dimensional black hole for small black holes do not depend on the surface gravity. This is of course different from asymptotically flat black holes. The presence of the AdS potential barrier at infinity is cited as the reason for this difference. Without going into the details of the numerics, we wish to point out the following : The numerical analysis of [74] concentrates on the near-horizon region. It is not clear then how such an analysis would reflect the properties of the AdS barrier at infinity. Assuming it does, it is natural to expect

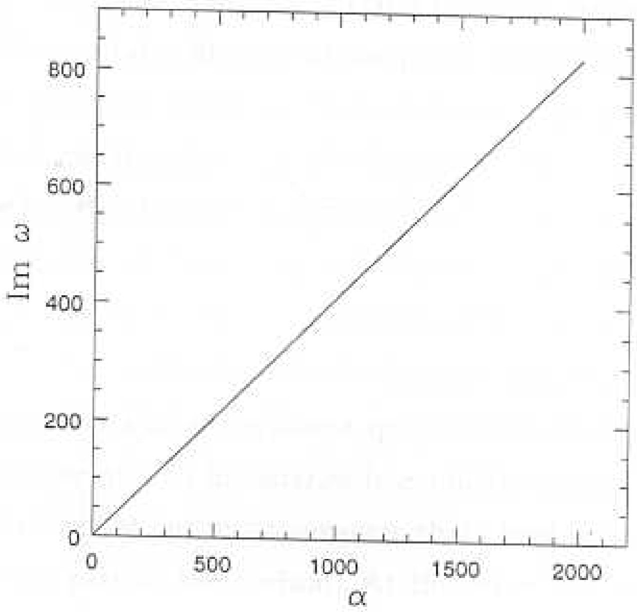

Fig. 3b

Figure 3b. *$Im(\omega)$ as a function of α*

that for *any* potential that behaves like the black hole potential at both the horizon and infinity (i.e has a potential barrier of the same form as a function of r_* and the same dependence on r_+ at both ends), the quasi-normal modes would behave in a similar manner. But that is not true. The simplest exactly solvable potentials similar to what we have used in our analysis for the BTZ black hole, but with α representing the surface gravity of this five dimensional black hole can be checked for this. The advantage is that for them, the solutions can be found exactly. They do not reflect the small r_+ behaviour found in [74]. Therefore, we feel that the numerical integration of [74] must be cross-checked by taking a test potential as suggested above, and seeing if it reproduces the behaviour of the exact solution, which is known.

A numerical computation of QN modes is tricky because of the nature of the boundary conditions on the mode solution at both the horizon and at infinity. The mode, which is ingoing (and not normalisable) at the horizon, could be contaminated by an outgoing component which goes to zero there. At the other boundary, the solution is required to go to zero. In a numerical truncation, it could also be contaminated as $x \to 0$ (i.e as $r \to \infty$) by the solution that blows up at this end. Therefore, in a numerical computation, it is essential to ensure the correct ingoing behaviour near the horizon and the correct *asymptotic* behaviour of the solution that goes to zero as $r \to \infty$. In our method, similar to the continued fraction method for asymptotically flat black holes, we have a *specific* ansatz for the wave function where the behaviour at *both* boundaries is explicitly present in the form of the ansatz. The form of our ansatz ensures that there is no contamination from the outgoing part at the horizon. At the other end as $x \to 0$ (i.e as $r \to \infty$), we *demand* that the solution must fall off as $x^{\frac{5}{2}}$ at every order. This *ensures* that there is no contamination from the solution that blows up at this end.

We have presented a new approach to computing the quasi-normal modes of AdS black holes. The novel feature of this method was an ansatz for the QN mode wave function which was derived from a superpotential. This was made in analogy with the case of the three dimensional BTZ black hole where the modes can be obtained exactly and the wave function is derived from a superpotential. The BTZ QN modes were proportional to the surface gravity. The modes obtained by us numerically for the five dimensional black hole are also approximately proportional to the surface gravity. More importantly, the modes obtained by us numerically are proportional to the inverse of the horizon radius for small black holes, reflecting the well-known fact that these black holes are unstable. We have also shown, from some scaling properties of the differential equation obeyed by the mode solutions, that this is indeed to be expected for small black holes. Work is in progress to compute the QN modes for AdS black holes in four and seven dimensions, and also the corresponding Reissner-Nordstrom black holes using this approach. Some preliminary work on the five dimensional RN AdS black hole seems to suggest that the QN mode increases with the charge of the black hole.

Chapter 6

Conclusions

The last three decades have seen extensive progress in our understanding of black hole physics. Recent developments like the AdS/CFT correspondence have related properties of black holes to those of gauge theories, motivating further research on black holes, particularly anti-deSitter black holes. However, some key questions still remain unanswered. The purpose of this thesis has been to extensively study *both* classical and quantum aspects of certain anti-deSitter black holes. The quantum aspects have been studied with a view to addressing the unanswered question of the origin of black hole entropy and also of quantum corrections to the semi-classical entropy. The classical aspects of AdS black holes studied in this thesis can be related to non-trivial features of strongly coupled gauge theories.

In the first chapter, we have studied aspects of black holes in anti-deSitter spacetime, and addressed the issue of a description of black hole entropy in terms of microscopic states. We have reproduced the semi-classical Bekenstein-Hawking entropy of the Euclidean BTZ black hole in the PRTV lattice gravity formalism in terms of states corresponding to various triangulations of the black hole manifold. We have obtained, in the second chapter, a closed form expression for the partition function of the Euclidean BTZ black hole, and seen that the next-order correction to the

Bekenstein-Hawking entropy is logarithmic in the black hole area. A correction of $-3/2 \log(area)$ was seen first for the Schwarzschild black hole in the canonical gravity formalism [7]. We obtain the correction with the same value of the coefficient, $-3/2$, as in [7]. The origin of this correction lies in the modular invariance of the partition function under modular transformations of the toral boundary. However, this correction is not seen in the PRTV lattice computation that we looked at earlier. This is due to the fact that the partition function derived from the PRTV formulation does not possess invariance under transformations of the boundary. Recently, a generalisation of the PRTV formulation for the case of a manifold with boundary has been proposed in [30] where the partition function is invariant under piece-wise linear (PL) homeomorphisms of the triangulation of the manifold, including those of the boundary. These homeomorphisms can be described by three elementary moves, the Pachner moves [75]. The proposed partition function can be thought of as an invariant for a three-manifold with boundary, under Pachner moves. This invariance under PL homeomorphisms for the triangulated manifold, for the case of the manifold boundary seems to be the discrete analogue of modular invariance. It would be very interesting if this could be proved. Possible future work could be also to obtain the BTZ black hole entropy using this partition function, and to see if the logarithmic correction to the semi-classical entropy is reproduced.

In the third and fourth chapter, we look at some classical aspects of black holes in anti-deSitter space. We study the modes of the dilaton field of supergravity in AdS black hole backgrounds. The spectrum of a certain class of equilibrium modes of the dilaton field in the infinite mass limit of the AdS-Schwarzschild black hole background reproduces the glueball spectrum of three-dimensional QCD. This has been understood as evidence in favour of the AdS/CFT correspondence. We have shown that the correct self-adjointness analysis reveals a discrete infinity of equilibrium modes in addition to those that correspond to the glueball spectrum. The interpretation of these modes for the boundary QCD is not clear. In the chapter, we have speculated on the possibility of it signifying the instability of the

QCD vacuum. There could however be another reason for these additional modes. There could be a problem with the way the infinite mass limit has been taken. This can be checked by following the spectrum of equilibrium modes of the dilaton as the infinite mass limit is being taken, and seeing if in the self-adjointness analysis, these modes still persist. This remains to be done. If they still persist, then they would indicate the kind of vacuum instability that we speculate about.

In the third chapter, we have also applied a self-adjointness analysis to scalar fields in the background of other non-extremal black holes. For these black holes, we seem to see a non-trivial time independent mode localised at the horizon. Interestingly enough, there is no such mode for the extremal RN black hole.

There are another class of well-studied modes of the scalar field in a black hole background. These are the quasi-normal modes. The quasi-normal modes of AdS black holes, whcich determine the time-scale of decay of a perturbation of the black hole, also describe, via the AdS/CFT conjecture, the time-scale of return to equilibrium of the Yang-Mills theory on the black hole boundary. We compute, in the fourth chapter, the quasi-normal modes of the BTZ black hole *exactly* and find that they are proportional to the surface gravity. This is the first instance of an exact computation of quasi-normal modes for a black hole. We also present a novel method, based on superpotentials, for computing these modes for AdS black holes in any dimension. We use the method to compute these modes for the five-dimensional AdS-Schwarzschild black hole. Again, the modes seem to be proportional to the surface gravity.

The computation of quasi-normal modes, particularly for the BTZ black hole, makes many issues accessible for study. One of these is the issue of black hole formation. Quasi-normal frequencies are characteristic frequencies associated with the black hole and determine the decay of any perturbation of the black hole. The formation of a black hole from collapsing matter is believed to be associated with a characteristic scaling of certain natural order parameters during the collapse process. This scaling, first seen by Choptuik [76] in the context of asymptotically flat black holes, is known as Choptuik scaling and there is also a scaling exponent associated with it.

One could then ask the following questions :

- *Are the quasi-normal modes of a black hole for perturbation by a scalar field, for e.g, related to the Choptuik scaling exponent for the formation of the black hole from collapse of scalar fields?*

- The quasi-normal modes for a black hole are different from those of a star. As a black hole has a horizon, it is necessary to put ingoing boundary conditions at the horizon. This has a physical meaning, as the black hole absorbs, and any perturbation will eventually decay. The black hole quasi-normal modes are therefore complex. *Can one follow the black hole formation process from the collapse of matter, and explicitly see the appearance of the complex quasi-normal mode as the black hole is formed ?*

- *Can the quasi-normal modes associated with gravitational perturbations be related to the black hole entropy ?* [1]

These questions have not been easy to address in the absence of *exact* quasi-normal mode solutions. However, we have computed the quasi-normal modes exactly for the BTZ black hole. Scenarios for the formation of a BTZ black hole from collapsing matter have been well studied. These include the formation of a BTZ black hole from the collision of two point particles [77], from the collapse of a spherical dust shell [78], and from scalar field collapse [79]. Therefore, the above questions could be addressed for the BTZ black hole. (The third question however, does not have much relevance in $(2+1)$ dimensions as there are no gravitational waves.) Following our work, a relationship between the quasi-normal modes and the Choptuik scaling exponent for the BTZ black hole has already been found [80]. However, the

[1] Discussions with R. Sorkin on this issue are gratefully acknowledged.

second question relating to the appearance of the quasi-normal mode in black hole formation needs to be answered.

These questions are also of interest as the AdS/CFT correspondence relates any process in the bulk space, like the formation of a black hole, to a corresponding process in the boundary. There has been some work in this direction [67, 81, 82], but answering the above questions could lead to interesting interpretations of the corresponding process in the Yang-Mills theory on the boundary.

In conclusion, the thesis has been a study of certain aspects of black holes in anti-deSitter space. This study has been used to successfully deal with issues related to black hole physics, and also to predict certain features for strongly coupled gauge theories related to the black holes via the AdS/CFT correspondence. The work in this thesis has also made it easier to address certain questions in black hole formation. However, many more issues remain to be resolved. We hope to be able to return to them in the future.

Chapter 7

Appendix 1 : $6j$ symbols

7.1 Definition and Orthogonality

This appendix is a short summary of some important results and properties of the Wigner $6j$ symbols. More details and useful references for these can be found in [83]. The Wigner $6j$ symbols are related to the coefficients of transformations between different coupling schemes of three angular momenta. Angular momenta j_1, j_2, j_3 may be coupled to give a resultant angular momentum j and its projection m in three ways:

I) $j_1 + j_2 = j_{12}, \quad j_{12} + j_3 = j,$

II) $j_2 + j_3 = j_{23}, \quad j_1 + j_{23} = j,$

III) $j_1 + j_3 = j_{13}, \quad j_{13} + j_2 = j.$

Let us consider first the coupling scheme I. A state $|j_1 j_2 (j_{12}) j_3 j m>$ can be written using the Clebsch-Gordon coefficients as

$$|j_1 j_2 (j_{12}) j_3 j m >= \sum_{m_1, m_2, m_3} C^{jm}_{j_{12} m_{12} j_3 m_3} C^{j_{12} m_{12}}_{j_1 m_1 j_2 m_2} |j_1 m_1, j_2 m_2, j_3 m_3 > . \quad (7.1)$$

Similarly, for the coupling scheme II, a state $|j_1 j_2 j_3 (j_{23}) j m >$

is written as

$$|j_1j_2j_3(j_{23})jm>= \sum_{m_1,m_2,m_3} C^{jm}_{j_1m_1j_{23}m_{23}} C^{j_{23}m_{23}}_{j_2m_2j_3m_3} |j_1m_1, j_2m_2, j_3m_3> . \quad (7.2)$$

Then the Wigner $6j$ symbol is defined by the relation

$$< j_1j_2(j_{12})j_3jm|j_1j_2j_3(j_{23})j'm' >= \delta_{jj'}\delta_{mm'}(-1)^(j_1 + j_2 + j_3 + j)$$
$$\sqrt{(2j_{12}+1)(2j_{23}+1)} \left\{ \begin{array}{ccc} j_1(t) & j_2(t) & j_3(t) \\ j_4(t) & j_5(t) & j_6(t) \end{array} \right\} \quad (7.3)$$

Thus, the $6j$ symbols can be written in terms of the Clebsch-Gordon coefficients

$$\sum C^{jm}_{j_{12}m_{12}j_3m_3} C^{j_{12}m_{12}}_{j_1m_1j_2m_2} C^{j'm'}_{j_1m_1j_{23}m_{23}} C^{j_{23}m_{23}}_{j_2m_2j_3m_3} = \delta_{jj'}\delta_{mm'}(-1)^{j_1+j_2+j_3+j}$$
$$\sqrt{(2j_{12}+1)(2j_{23}+1)} \left\{ \begin{array}{ccc} j_1 & j_2 & j_3 \\ j_4 & j_5 & j_6 \end{array} \right\} \quad (7.4)$$

here the sum is over m_1, m_2, m_{12}, m_{23} while m and m' are fixed.

The arguments of the $6j$ symbol are integer or half-integer non-negative numbers. They obey orthgonality and normalisation conditions like

$$\sum_{j_{12}} \sqrt{(2j_{12}+1)(2j_{23}+1)} \left\{ \begin{array}{ccc} j_1 & j_2 & j_{12} \\ j_3 & j & j_{23} \end{array} \right\} \left\{ \begin{array}{ccc} j_1 & j_2 & j_{12} \\ j_3 & j & j'_{23} \end{array} \right\} = \delta_{j_{23}j'_{23}} \quad (7.5)$$

7.2 The $6j$ symbol in Terms of a Finite Sum

The $6j$ symbols $\left\{ \begin{array}{ccc} a & b & c \\ d & e & f \end{array} \right\}$ vanish if any of the triads (abc), (cde), (aef) and (bdf) do not obey triangle inequalities between themselves. If they do, then one can write an expression for the $6j$ symbol in terms of a finite sum. First we define

$$\Delta(abc) = \left[\frac{(a+b+c)!(a-b+c)!(-a+b+c)!}{(a+b+c+1)!}\right]^{\frac{1}{2}} \tag{7.6}$$

Then, the $6j$ symbol is given by the following formula :

$$\left\{\begin{matrix} a & b & c \\ d & e & f \end{matrix}\right\} = \Delta(abc)\Delta(cde)\Delta(aef)\Delta(bdf)$$

$$\times \sum_n \frac{(-1)^n(n+1)!}{(n-a-b-c)!(n-c-d-e)!(n-b-d-f)!(a+b+d+e-n)!} \\ \times(a+c+d+f-n)!(b+c+e+f-n)! \tag{7.7}$$

Here, the sum over n is over all integer nonnegative n such that no factorial in the denominator has a negative argument.

Using this formula, one can obtain an asymptotic expression for the $6j$ symbol valid when three of the spins are large, i.e $d = e = f = R > 1$

$$\left\{\begin{matrix} a & b & c \\ R & R & R \end{matrix}\right\} \approx \frac{(-1)^c}{\sqrt{2R(2c+1)}} C^{c0}_{a0b0} \tag{7.8}$$

where C^{c0}_{a0b0} is the Clebsch-Gordon coefficient.

7.3 $SU(2)_q - 6j$ symbols

To define $SU(2)_q - 6j$ symbols, we first define q numbers. A discussion on q numbers and their relation to quantum groups is found in [84]. In this appendix, we merely state the expression for the $SU(2)_q - 6j$ symbol in terms of a finite sum as before.

The q-number of an integer n is

$$[n] = \frac{q^{n/2} - q^{-n/2}}{q^{1/2} - q^{-1/2}} \tag{7.9}$$

The factorial of a q-number is defined in the usual way, i.e $[n]! = [n][n-1].....[2][1]$.

We are interested in the case when $q = \exp \frac{2\pi i}{k+2}$, where k is an integer. We can define the q-analog of (7.6) which is as follows :

$$\Delta_q(abc) = \left[\frac{[a+b+c]![a-b+c]![-a+b+c]!}{[a+b+c+1]!} \right]^{\frac{1}{2}} \tag{7.10}$$

This formula is similar to (7.6) except that ordinary numbers are replaced by q numbers. Again, (7.10) is defined only when the triangle inequalities $a \leq b+c$, $b \leq a+c$, $c \leq a+b$ are satisfied; in addition, there is a restriction that $a+b+c$ is an integer that is less than or equal to k.

Now we can write the q-analog of (7.7) which is

$$\begin{Bmatrix} a & b & c \\ d & e & f \end{Bmatrix}_q = \Delta_q(abc)\Delta_q(cde)\Delta_q(aef)\Delta_q(bdf)$$

$$\times \sum_n \frac{(-1)^n [n+1]!}{([n-a-b-c]![n-c-d-e]![n-b-d-f]![a+b+d+e-n]! \times [a+c+d+f-n]![b+c+e+f-n]!)} \tag{7.11}$$

For k large, we see from the expression (7.9) that the q-number tends to the ordinary number. Therefore, the $SU(2)_q - 6j$ symbol also reduces to the ordinary $6j$ symbol.

Chapter 8

Appendix 2 : Self-adjoint operators

In this appendix, we summarise some useful definitions and results involving self-adjoint operators. Proofs of the results and other details are found in [61, 62] .

Adjoint of an operator :

A discussion of self-adjointness for an unbounded operator $\mathcal{O}$ first requires us to define the domain $D(\mathcal{O})$ of $\mathcal{O}$. We will only be interested in operators that are defined on domains that are dense in the Hilbert space. This allows us to define the Hilbert space adjoint of an operator $\mathcal{O}$ on a Hilbert space $\mathcal{H}$ and also the domain of the adjoint $D(\mathcal{O})$. If $x, y \in \mathcal{H}$, then the adjoint $\mathcal{O}^*$ of the operator $\mathcal{O}$ satisfies $(x, \mathcal{O}y) = (\mathcal{O}^* x, y)$, where $(.,.)$ is the inner product on the Hilbert space.

Definition of a Hermitian operator :

A densely defined operator $\mathcal{O}$ on $\mathcal{H}$ is called symmetric, or

Hermitian if for all $\phi \in D(O)$, $\mathcal{O}\phi = \mathcal{O}^*\phi$ and $D(\mathcal{O}) \subset D(\mathcal{O}^*)$. This is equivalent to the more familiar condition $(\mathcal{O}\phi, \psi) = (\phi, \mathcal{O}\psi)$ for all $\phi, \psi \in D(\mathcal{O})$.

Definition of a self-adjoint operator :

$\mathcal{O}$ is self-adjoint if and only if $\mathcal{O}$ is Hermitian and $D(\mathcal{O}) = D(\mathcal{O}^*)$.

Criteria for self-adjointness - Deficiency indices :

One can check for the self-adjointness of a Hermitian operator by studying its "deficiency indices", which are defined as follows. Let $\mathcal{K}_\pm = Ker(i \pm \mathcal{O}^*)$, where $Ker(X)$ is the kernel of the operator X. The integers $n_\pm \equiv dim\ \mathcal{K}_\pm$ are the deficiency indices of the operator. If $n_\pm = 0$, then $\mathcal{O}$ is self-adjoint. If $n_+ = n_- = n \neq 0$, then $\mathcal{O}$ can be extended to a self-adjoint operator. Different self-adjoint extensions of the operator are in one-to-one correspondence with unitary maps from $\mathcal{K}_+$ to $\mathcal{K}_-$, that is, they are labeled by a $U(n)$ matrix. A self-adjoint extension involves adding appropriate vectors to $D(\mathcal{O})$ such that $\mathcal{O}$ remains Hermitian, and now, $D(\mathcal{O}) = D(\mathcal{O}^*)$. If $n_+ \neq n_-$, then this cannot be done, and $\mathcal{O}$ cannot be made self-adjoint.

Properties of self-adjoint operators :

- All eigenvalues of a self-adjoint operator are real.
- Eigenvectors belonging to different eigenvalues are orthogonal.
- The eigenvectors form a complete set.

Bibliography

1. S. W. Hawking, Phys. Rev. Lett. **26**, 1344 (1971).
2. J. D. Bekenstein, Phys. Rev. **D7**, 2333 (1973); Phys. Rev. **D9**, 3292 (1974).
3. J. M. Bardeen, B. Carter and S. W. Hawking, Comm. Math. Phys. **31**, 161 (1973).
4. S. W. Hawking, Comm. Math. Phys. **43**, 199 (1975).
5. A. Peet, *TASI Lectures on black holes in string theory*, hep-th/0008241.
6. M. Banados, C. Teitelboim and J. Zanelli, Phys. Rev. Lett. **69**, 1849 (1992);

   M. Banados, M. Henneaux, C. Teitelboim and J. Zanelli, Phys. Rev. **D48**, 1506 (1993).
7. R. K. Kaul and P. Majumdar, Phys. Rev. Lett. **84**, 5255 (2000).
8. G. Ponzano and T. Regge *in* Spectroscopic and group theoretical methods in physics, ed. F.Block (North-Holland, Amsterdam, 1968).
9. V. G. Turaev and O. Y. Viro, Topology **31**, 865 (1992).
10. V. Suneeta, R. K. Kaul and T. R. Govindarajan, Mod. Phys. Lett. **A14**, 349 (1999).
11. S. Carlip, Class. Quant. Grav. **17**, 4175 (2000).
12. A. Ashtekar, J. Baez, A. Corichi and K. Krasnov, Phys. Rev. Lett.**80**, 904 (1998.)

13. R. K. Kaul and P. Majumdar, Phys. Lett. **B439**, 267 (1998).

14. T. R. Govindarajan, R. K. Kaul and V. Suneeta, Class. Quant. Grav. **18**, 2877 (2001).

15. A review can be found in O. Aharony, S. S. Gubser, J. Maldacena, H. Ooguri and Y. Oz, Phys. Rept. **323**, 183 (2000).

16. J. Polchinski, String Theory, Vols. I and II (Cambridge University Press, 1998).

17. E. Witten, Adv. Theor. Math. Phys. **2**, 253 (1998).

18. E. Witten, Adv. Theor. Math. Phys. **2**, 505 (1998).

19. S. W. Hawking and D. Page, Commun. Math. Phys. **87** 577 (1983).

20. T. R. Govindarajan, V. Suneeta and S. Vaidya, Nucl. Phys. **B583**, 291 (2000).

21. T. R. Govindarajan and V. Suneeta, Class. Quant. Grav. **18**, 265 (2001).

22. S. Carlip and C. Teitelboim, Phys. Rev.**D51**, 622 (1995).

23. T. Regge, Nuovo Cimento **19** 558 (1961).

24. H. Ooguri, Nucl. Phys.**B382**, 276 (1992).

25. A. Achucarro and P. Townsend, Phys. Lett. B **180**, 89 (1986).

26. E. Witten, Nucl. Phys.**B311**, 46 (1989).

27. S. Mizoguchi and T. Tada, Phys. Rev. Lett.**68**, 1795 (1992).

28. H. Ooguri and N. Sasakura, Mod. Phys. Lett.**A6**, 3591 (1991).

29. L. Freidel and K. Krasnov, Class. Quant. Grav. **16**, 351 (1999).

30. G. Carbone, M. Carfora and A. Marzuoli, Commun. Math. Phys. **212**, 571 (2000).

31. C. Rovelli, Phys. Rev.**D48**, 2702 (1993).

32. G. Immirzi, Class. Quant. Grav. **14**, L177 (1997).

33. C. Rovelli and T. Thiemann, Phys. Rev. **D57** 1009 (1998).

34. S. Elitzur, G. Moore, A. Schwimmer and N. Seiberg, Nucl. Phys. B **326**, 10 8 (1989).

35. W. Ogura, Phys. Lett. **B229**, 61 (1989);
S. Carlip, Nucl. Phys. B **362**, 111 (1991).

36. D. Cangemi, M. Leblanc and R. Mann, Phys. Rev. **D48**, 3606 (1993).

37. J. M. F. Labastida and A. V. Ramallo, Phys. Lett. **B 227**, 92 (1989).

38. J. M. Isidro, J. M. F. Labastida and A. V. Ramallo, Nucl. Phys. B **398**, 1 87 (1993).

39. N. Hayashi, Prog. Theor. Phys. Suppl. **114**, 125 (1993).

40. J. D. Brown, G. L. Comer, E. A. Martinez, J. Melmed, B. F. Whiting and J. W. York, Class. Quant. Grav. **7**, 1433 (1990).

41. R. Mann and S. Solodukhin, Phys. Rev. **D55**, 3622 (1997).

42. S. Carlip, Phys. Rev. **D55**, 878 (1997).

43. J. Maldacena and A. Strominger, JHEP **9812** 005 (1998).

44. S. Chandrasekhar, The Mathematical Theory of Black Holes (Clarendon Press, Oxford, 1983).

45. R. Wald. J. Math. Phys **21**, 2802 (1980).

46. G. T. Horowitz, D. Marolf, Phys. Rev. **D52**, 5670 (1995).

47. C. Csáki, H. Ooguri, Y. Oz, J. Terning, JHEP **9901**, 017 (1999).

48. R. Koch, A. Jevicki, M. Mihailescu, J. P. Nunes, Phys.Rev. **D58**, 105009 (1998).

49. R. C. Brower, S. D. Mathur, C. Tan, Nucl. Phys. **B574**, 219 (2000).

50. S. Kalyana Rama and B. Sathiapalan, Mod. Phys. Lett. **A14**, 2635 (1999).

51. G. T. Horowitz, V. Hubeny, Phys. Rev. **D62**, 024027 (2000).

52. G. K. Savvidy, Phys. Lett. **71B**, 133 (1977).

53. H. B. Nielsen and M. Ninomiya, Nucl. Phys. **B156**, 1 (1979).

54. N. K. Nielsen and P. Olesen, Nucl. Phys. **B144**, 376 (1978).

55. J. Ambjørn, N. K. Nielsen and P. Olesen, Nucl. Phys. **B152**, 75 (1979).

56. E. Witten. Phys.Rev. **D44**, 314 (1991).

57. T. Jacobson. Phys. Rev. **D57**, 4890 (1998).

58. K. D. Kokkotas, B. Schmidt, Living Reviews in Relativity, **Vol.2** (1999). www.livingreviews.org/Articles/Volume2/1999-2kokkotas

59. H. Nollert, Class. Quant. Grav. **16**, R159 (1999).

60. S. Chandrasekhar, Proc. Roy. Soc. London **Ser.A392**, 1 (1984).

61. M. Reed and B. Simon, Methods of Modern Mathematical Physics, volume I. Functional Analysis (Academic Press, New York, 1972).

62. M. Reed and B. Simon, Methods of Modern Mathematical Physics, volume II. Fourier Analysis, Self-Adjointness (Academic Press, New York, 1975).

63. K. Meetz, Nuovo Cimento **34**, 690 (1964).

64. H. Narnhofer, Acta Physica Austriaca **40**, 306 (1974).

65. D. Kay, Phys. Rev.**D29**, 2409 (1984).

66. C. V. Vishveshvara, Nature **227**, 936 (1970)

67. U. H. Danielsson, E. Keski-Vakkuri and M. Kruczenski, JHEP **0002**, 039 (2000)

68. H-P. Nollert and B. G. Schmidt, Phys. Rev. **D45**, 2617 (1992)

69. B. F. Schutz and C. M. Will, Astrophys. J. **291**, L33 (1985)

70. E. W. Leaver, Proc. Roy. Soc. London, **Ser.A 402**, 285 (1985)

71. V. Ferrari and B. Mashhoon, Phys. Rev. **D30**, 295 (1984)

72. H-J. Blome and B. Mashhoon, Phys. Lett. **A 100**, 231 (1983)

73. F. Cooper, A. Khare and U. Sukhatme, Phys. Rep **251**, 267 (1995) .

74. J-M. Zhu, B. Wang and E. Abdalla, Phys. Rev. **D63**, 124004 (2001).

75. U. Pachner, Discr. Math. **81**, 37 (1990).

76. M. Choptuik, Phys. Rev. Lett. **70**, 9 (1993).

77. H-J. Matschull, Class. Quant. Grav. **16**, 1069 (1999).

78. Y. Peleg and A. Steif, Phys. Rev. **D51**, R3992 (1995).

79. F. Pretorius and M. Choptuik, Phys. Rev. **D62**, 124012 (2000).

80. D. Birmingham, *Choptuik scaling and quasi-normal modes in the AdS/CFT correspondence*, hep-th/0101194.

81. V. Balasubramanian and S. F. Ross, Phys. Rev. **D61**, 044007 (2000).

82. J. Louko, D. Marolf and S. F. Ross, Phys. Rev. **D62**, 044041 (2000).

83. D. A. Varshalovich, A. N. Moskalev and V. K. Khersonskii, *Quantum Theory of Angular Momentum* (World Scientific, 1988).

84. V. Chari and A. Pressley, *A Guide to Quantum Groups* (Cambridge University Press, 1994).